

Review

Breaking the Barrier: Strategies for Mitigating Shuttle Effect in Lithium–Sulfur Batteries Using Advanced Separators

Yingbao Zhu ¹, Zhou Chen ^{1,*} , Hui Chen ², Xuguang Fu ², Desire Emefa Awuye ³, Xichen Yin ¹ and Yixuan Zhao ¹

¹ School of Mechanical and Power Engineering, Nanjing Tech University, Nanjing 211800, China; 202161207212@njtech.edu.cn (Y.Z.); 202261107032@njtech.edu.cn (X.Y.); 202021106006@njtech.edu.cn (Y.Z.)

² Jiangsu Zhongneng Polysilicon Technology Development Co., Ltd., Xuzhou 221000, China; liuhui@gcl-power.com (H.C.); fuxuguang@gcl-power.com (X.F.)

³ Department of Minerals and Materials Engineering, University of Mines and Technology, Tarkwa 03123, Ghana; deawuye@umat.edu.gh

* Correspondence: zchen6240@njtech.edu.cn

Abstract: Lithium–sulfur (Li-S) batteries are considered one of the most promising energy storage systems due to their high theoretical capacity, high theoretical capacity density, and low cost. However, challenges such as poor conductivity of sulfur (S) elements in active materials, the “shuttle effect” caused by lithium polysulfide, and the growth of lithium dendrites impede the commercial development of Li-S batteries. As a crucial component of the battery, the separator plays a vital role in mitigating the shuttle effect caused by polysulfide. Traditional polypropylene, polyethylene, and polyimide separators are constrained by their inherent limitations, rendering them unsuitable for direct application in lithium–sulfur batteries. Therefore, there is an urgent need for the development of novel separators. This review summarizes the applications of different separator preparation methods and separator modification methods in lithium–sulfur batteries and analyzes their electrochemical performance.

Keywords: lithium–sulfur batteries; shuttle effect; separator; separator modification



Citation: Zhu, Y.; Chen, Z.; Chen, H.; Fu, X.; Awuye, D.E.; Yin, X.; Zhao, Y. Breaking the Barrier: Strategies for Mitigating Shuttle Effect in Lithium–Sulfur Batteries Using Advanced Separators. *Polymers* **2023**, *15*, 3955. <https://doi.org/10.3390/polym15193955>

Academic Editors: Yan Wang and Pengfei Qi

Received: 4 September 2023

Revised: 27 September 2023

Accepted: 27 September 2023

Published: 30 September 2023



Copyright: © 2023 by the authors. Licensee MDPI, Basel, Switzerland. This article is an open access article distributed under the terms and conditions of the Creative Commons Attribution (CC BY) license (<https://creativecommons.org/licenses/by/4.0/>).

1. Introduction

With the rising demand for electric vehicles and portable electronic devices, it is important to research and develop energy storage systems with high energy density, low cost, and extended service life [1]. Traditional lithium batteries are widely used due to their high working voltage, long cycle life, and good stability [2]. However, the high production cost, theoretical specific capacity, and low energy density of the electrode material make it difficult for traditional lithium batteries to meet the increasing market scale [3]. Lithium-sulfur (Li-S) batteries are regarded as one of the energy storage systems with great potential due to its low production cost, high theoretical specific capacity and energy density, abundant S elements in nature, and low toxicity [4]. They are also facing great challenges, such as the poor conductivity of S elements, the volume expansion of the cathode material, and the shuttle effect caused by lithium polysulfide in the commercial development of Li-S [5,6]. Solving the above problems is crucial for the commercialization of lithium-sulfur batteries.

Li-S batteries are composed of an anode, a cathode, an electrolyte, and a separator, as shown in Figure 1, which represents a schematic diagram of a typical Li-S battery, in which the separator plays a key role in solving the shuttle effect of lithium polysulfide [7,8]. The shuttle effect occurs because lithium polysulfide is easily soluble in the electrolyte and moves between the cathode and the anode, resulting in irreversible volume loss [9]. Therefore, studying a separator with excellent performance is very important in order to solve the shuttle effect.

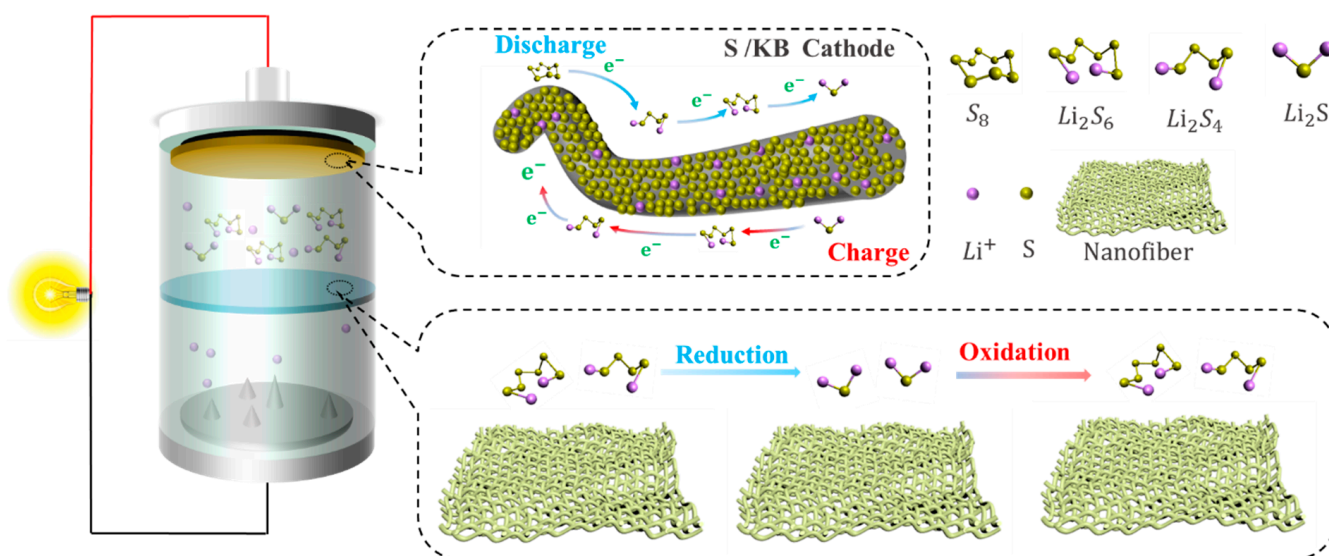


Figure 1. Lithium–sulfur battery model separator.

As shown in Figure 2a, the gray color in the histogram represents the number of publications (A), corresponding to the left axis. The orange histogram represents Publication B, and the quantity corresponds to the right axis. The number of publications on Li-S separators has increased year by year, and this shows that Li-S separators have been a research hotspot in this field.

At present, commercial Li-S separators mainly consist of PP and PE separators [10], which are widely used in Li-S due to their good chemical stability and good mechanical strength. However, this type of separator has a weak ability to inhibit the shuttle effect of polysulfides, poor affinity with electrolytes, and low porosity, resulting in poor battery performance, so this type of olefin separator is not well used in Li-S [11].

To suppress the shuttle effect in Li-S, it is necessary to study a new type of separator with good performance or to modify the original commercial separator. Figure 2b shows the main development history of lithium–sulfur batteries. In recent years, there has been a proliferation of comprehensive reviews on lithium–sulfur battery separators. However, these reviews tend to be confined to specific fabrication techniques such as electrospinning, deposition methods, or filtration processes. In contrast, this study not only encompasses an overview of conventional methods for fabricating lithium–sulfur battery separators and their applications in lithium–sulfur batteries, but also extends its scope to include composite fabrication processes and their potential applications in lithium–sulfur batteries. This paper reviews the lithium–sulfur battery separators prepared by different preparation or modification methods in recent years, which inhibit the shuttle effect of polysulfides and improve the electrochemical performance. Finally, future research directions involving lithium–sulfur batteries are analyzed, and the prospect of building high-performance lithium–sulfur batteries is introduced.

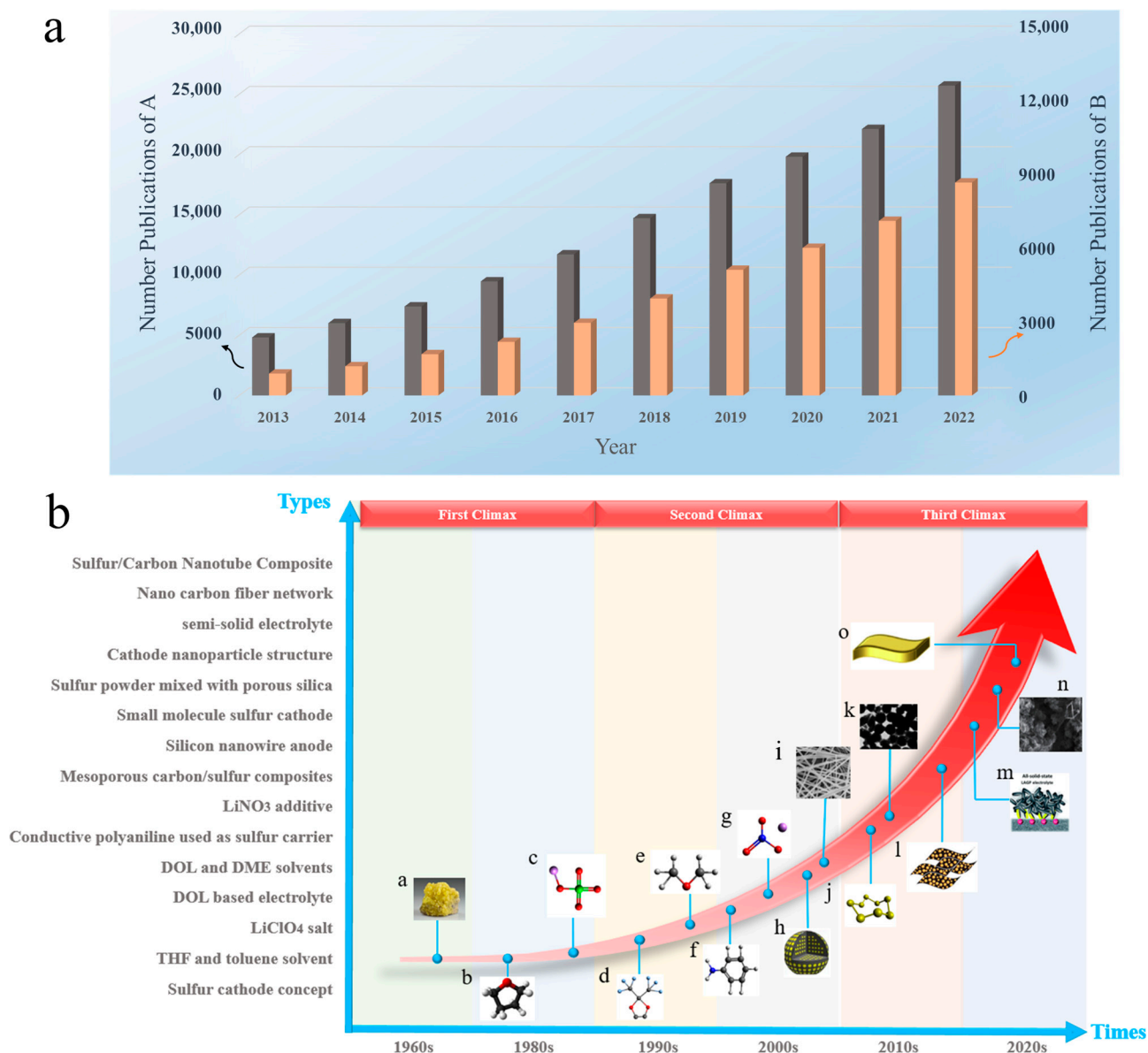


Figure 2. Lithium–sulfur battery development history: (a) Publications A and B in the past decade by searching for “lithium–sulfur battery separator” and “lithium–sulfur battery” as “keywords” on the Google Scholar website. (b) The development history of lithium–sulfur batteries: (a) sulfur cathode concept; (b) THF and toluene solvent; (c) LiClO₄ salt; (d) DOL-based electrolyte; (e) DOL and DME solvents; (f) conductive polyaniline used as sulfur carrier; (g) LiNO₃ additive; (h) mesoporous carbon/sulfur composites; (i) silicon nanowire anode; (j) small molecule sulfur cathode; (k) sulfur powder mixed with porous silica; (l) cathode nanoparticle structure; (m) semi-solid electrolyte; (n) nano carbon fiber network; (o) sulfur/carbon nanotube composite [12–16]. Reproduced with permission from the Particle & Particle Systems Characterization and Journal of Materials Chemistry A and Nano Research and Energy and Royal Society Of Chemistry.

2. The Working Principle and Problems of Li-S

2.1. Working Mechanism of Li-S

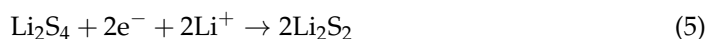
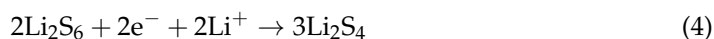
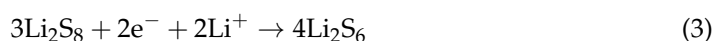
The electrochemical reactions that occur in Li-S are different from traditional lithium batteries [17], and the redox reaction during the charging and discharging of Li-S involves the conversion between different valence ions of the S atom, making it more complex than traditional lithium-ion batteries [18,19]. Lithium–sulfur batteries generally consist

of a lithium metal negative electrode, an organic liquid electrolyte, and a sulfur–carbon composite positive electrode [20]. Taking a positive electrode material such as sulfur elemental as an example, during discharge, the lithium metal of the anode is oxidized to generate electrons and lithium ions, and the lithium ions diffuse to the cathode through the electrolyte. At the same time, the electrons move to the sulfur element of the cathode through the external circuit, the sulfur element is reduced to S^{2-} , and S^{2-} and Li^+ generate Li_2S at the cathode [21]. During the discharge process, when the sulfur element in the cathode reacts completely with the lithium ion, the total equation of the electrochemical reaction is as follows:



As shown in Figure 3a, the spatial structure of elemental sulfur is formed by eight sulfur atoms connected by covalent bonding, so there are multiple cleavage and bonding sites of S-S bonds in sulfur elements, resulting in more complex redox reactions in the charging and discharging process of Li-S [20,22]. At present, there are many studies on the S conversion of lithium–sulfur battery charging and discharging process [22,23]. According to the measurement of the electrolyte mass spectrometry (LC/MS) of different charges and discharges, the reduction reaction of elemental sulfur is carried out in multiple steps, and there are a variety of different intermediate products, such as Li_2S_8 , Li_2S_6 , Li_2S_4 , Li_2S_2 , Li_2S_2 , and Li_2S [24].

When discharging, the electrochemical reaction is as formulated (2)–(6) [17]:



As can be seen in Figure 3b, it can be seen from the discharge curve of the Li-S that there are two discharge platforms in the discharge process [25]. The high discharge platform is between 2.3~2.4 V; at this time, the S_8 product is a variety of soluble long-chain lithium polysulfide Li_2S_x ($4 \leq x \leq 8$) [26]. The low discharge platform is between 1.8~2.1 V; at this time, the corresponding long-chain lithium polysulfide Li_2S_x ($4 \leq x \leq 8$) is further reduced to short-chain lithium polysulfide Li_2S_x ($1 \leq x \leq 4$) [27] (Wu et al. [28]). According to experimental calculations, the utilization rate of the active material of the high discharge platform is only 25%, and the theoretical capacity of the process is 418 mAh g^{-1} . The active material utilization rate of the low discharge platform is 75%, and the theoretical capacity of the process is 1254 mAh g^{-1} . At the low discharge platform, due to the growth of lithium dendrites and phase transition processes, the reaction kinetics of this process slow down, and the actual discharge-specific capacity of the battery is lower than the theoretical capacity, so the actual specific capacity of the Li-S is lower than the theoretical specific capacity throughout the entire discharge process [29–32].

When charging, there is only one noticeable platform of about 2.4 V [33]. Electrochemical reactions can be described by Formulas (7) and (8):



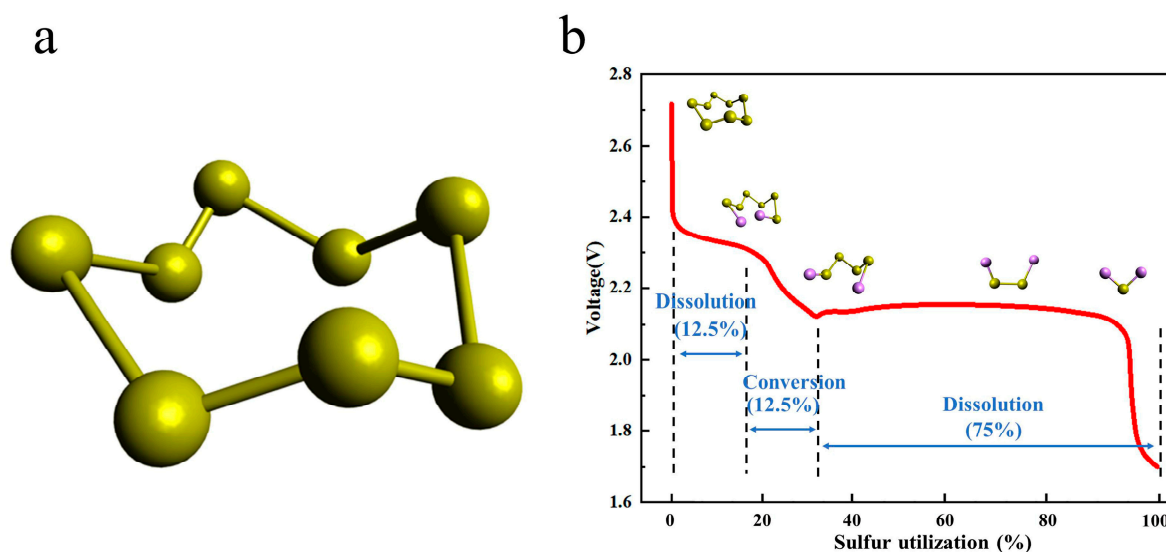


Figure 3. (a) Schematic diagram of the spatial structure of elemental sulfur. (b) Red is the discharge curve of lithium-sulfur battery, showing the sulfur electrode utilization [28]. Reproduced with permission from American Chemical Society.

2.2. The Existing Problems of Li-S

2.2.1. Cathode

Because sulfur resources are abundant, non-toxic, and non-polluting; the theoretical specific capacity is 1675 mAh g^{-1} ; and they have low prices and other advantages, sulfur was selected as the cathode material in Li-S batteries [34–36]. However, problems such as low conductivity, volume expansion during electrochemical reactions, and shuttle effect lead to low coulombic efficiency, and the actual specific capacity is much lower than the theoretical specific capacity, in addition to poor cycle stability [37], as shown in Figure 4. Among these, the shuttle effect [38,39] is the most important factor for the short cycle life and low specific capacity of Li-S. The solution to these problems is crucial for the commercialization of Li-S. Wang et al. [40] synthesized sulfur particles coated with PEG surfactants and wrapped them in carbon-black-decorated graphene oxide flakes in a simple assembly process. The graphene-sulfur composite showed a relatively stable specific capacity of about 600 mAh g^{-1} and attenuation of less than 15% in 100 cycles. Yang et al. [36] used boron-doped porous carbon material as the host material of the S cathode. B-doped carbon material exhibits higher conductivity than pure porous carbon. At 0.25 C, the S/B doped carbon cathode can provide a higher initial capacity of 1300 mAh g^{-1} compared to the cathode based on pure porous carbon. The cycle stability and rate capability are also improved.

2.2.2. Separator

As a vital part of Li-S, separators play a great role in the performance of Li-S [41]. During the charging and discharging process of lithium-sulfur batteries, the separator does not directly participate in the electrochemical reaction of mutual conversion between polysulfides [42]. However, the wettability, thermal stability, mechanical properties, porosity, liquid absorption rate, and other properties of the separator affect the specific capacity and cycle life of the Li-S, as shown in Figure 4. As a separator for Li-S, it is not only necessary to maintain the advantages of wettability, thermal stability, mechanical properties, porosity, and liquid absorption rate [43], but also to effectively suppress the shuttle effect [44].

With the development of clean energy, traditional separators such as polypropylene, polyethylene, and polyimide are widely employed in lithium-ion batteries. However, due to the distinct operational mechanisms of lithium-ion batteries and lithium-sulfur batteries, these traditional separators present certain challenges when applied in lithium-sulfur

battery systems. Primarily, the major issue lies in the inability of traditional separators to impede the shuttle effect of polysulfides. Owing to the relatively large pores in conventional separators, polysulfides can readily permeate, leading to diminished battery capacity and low Coulombic efficiency. Secondly, traditional polypropylene and polyethylene separators exhibit inadequate resistance to high temperatures, posing safety risks under elevated operating temperatures. Polyimide separators suffer from suboptimal mechanical properties, rendering them susceptible to lithium dendrite penetration and associated safety concerns.

2.2.3. Anode

The weight density is low, and the theoretical specific capacity is 3860 mAh g^{-1} higher [45]. Due to its low reduction potential [46,47] and other advantages, lithium metal was chosen as the electrode material for Li-S. Metallic lithium is used as an anode in Li-S [48] due to the growth of lithium dendrites [40,49–51]. Lithium dendrites easily pierce the separator, resulting in potential safety hazards in the circuit. Lithium metal itself has strong activity and can easily have side reactions with electrolytes, resulting in low battery cycle life and other problems that limit the commercial development of Li-S, as shown in Figure 4. At present, in response to the existing problems of anode lithium metal, a large number of researchers focus on electrolyte additives and lithium anode surface to form a protective film (artificial SEI film) [52–54] and explore several aspects of other materials that can replace metal lithium anodes. To inhibit the growth of lithium dendrites on the anodes of Li-S, Guo et al. [55] used VC-LiNO as an electrolyte additive and an efficiency of lithium plating/stripping up to 100%, resulting in a uniform and stable SEI separator with high ionic conductivity (Li et al. [56]). The artificial Li_3PO_4 SEI layer was prepared, which effectively inhibited the growth of lithium dendrites and had good chemical stability (Jan et al. [57]). Si-C and hard carbon anodes were prepared, which improved the cycle stability of the battery. The Coulombic efficiency of more than one thousand cycles was higher than 99%, and the attenuation of each cycle capacity was only 0.08%.

2.2.4. Electrolyte

Electrolytes, as a pivotal constituent bridging the positive and negative electrodes, wield substantial influence on the transport of lithium ions, thereby exerting a direct impact on the performance of lithium–sulfur batteries. Electrolytes can be classified into two categories: liquid electrolytes and solid electrolytes.

Presently, liquid electrolytes find extensive application in lithium–sulfur batteries, primarily owing to their facile synthesis, high ionic conductivity, and favorable chemical stability. Nevertheless, liquid electrolytes are not without their challenges. Firstly, at the positive electrode, liquid electrolytes tend to dissolve polysulfides, which subsequently diffuse through the electrolyte to the negative electrode, leading to diminished Coulombic efficiency and corrosion of the lithium negative electrode. Secondly, liquid electrolytes typically comprise flammable organic solvents, thus posing safety concerns when exposed to elevated temperatures. In response to these issues associated with liquid electrolytes, a substantial body of researchers is actively engaged in addressing these challenges. This includes the modification of electrolyte composition, the exploration of novel multi-component solvents, and the incorporation of functional additives [58].

The application of solid-state electrolytes effectively mitigates the “shuttle effect” caused by the dissolution of polysulfides while also eliminating flammable organic solvents, thereby significantly enhancing the safety of lithium–sulfur batteries. However, current lithium–sulfur batteries employing solid-state electrolytes still face challenges such as low ionic conductivity and high interfacial impedance, which impede the further advancement of solid-state electrolyte technology. To address these issues, ongoing research efforts are predominantly focused on the development of novel functional materials and the exploration of inorganic fillers as strategies to tackle these challenges.

2.2.5. Binders

Binders, constituting an integral part of the sulfur cathode in lithium–sulfur batteries, serve the crucial function of ensuring effective electrochemical contact among the conductive agent, sulfur, and current collector. Moreover, they mitigate volumetric variations of active materials during cycling. Binders play a pivotal role in lithium–sulfur batteries, and the commonly utilized types encompass polymeric, bio-based, and inorganic binders. Challenges regarding binders encompass inadequate mechanical properties and the detachment of electrode materials during cycling, consequently leading to a diminished cycling lifespan and reduced stability of the battery. In the future, bio-based binders exhibiting natural, renewable, and superior adhesive properties hold substantial promise for advancement, thus augmenting lithium–sulfur batteries [59].

2.2.6. Current Collector

Aluminum foil has found widespread application as a current collector for sulfur cathodes. However, at elevated temperatures, aluminum and sulfur can undergo reactions, which may pose safety concerns. Presently, the use of carbon-coated aluminum foil is employed to mitigate direct contact between sulfur and aluminum foil, thereby enhancing the safety of lithium–sulfur batteries. The presence of carbon coatings effectively improves the adhesion between the active materials and the current collector, while simultaneously enhancing electrical conductivity [60].

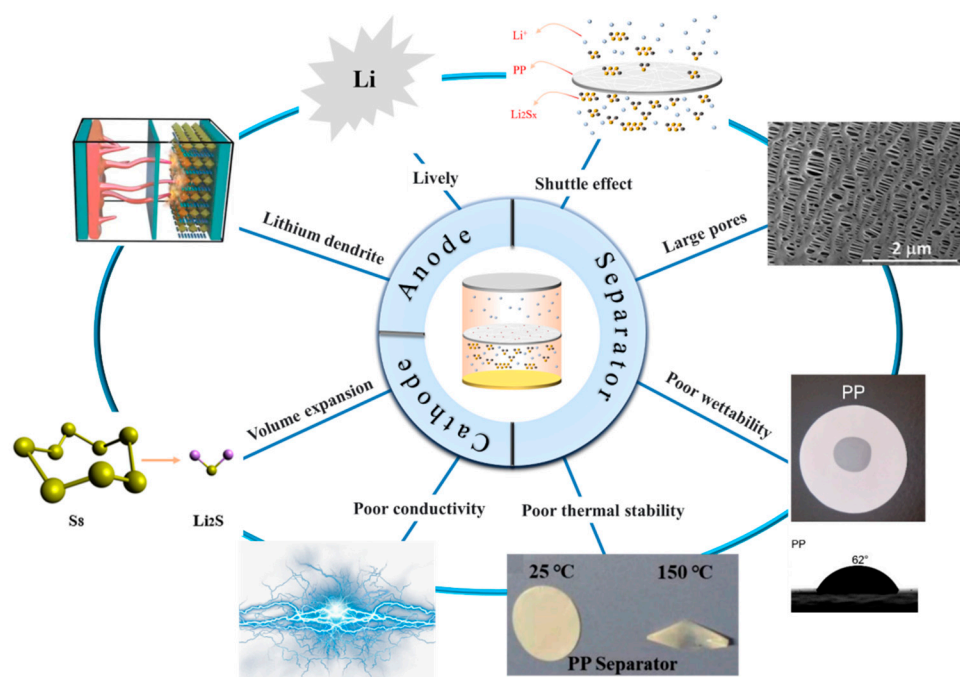


Figure 4. Existing problems with lithium–sulfur batteries [61]. Reproduced with permission from the Polymers.

3. Methods

With the development of science and technology, separator technology has also been continuously developed and updated, and the methods of preparing polymer separators have also been diversified. Different preparation methods can be selected according to the material properties and separator application direction. The battery separator film is closely related to the energy density, stability, and cycle life of the battery [62]. A battery separator composed of nanofibers has the advantages of a large specific area and high porosity [63], which has attracted close attention. There are many methods of separators, but electrospinning [64], vacuum filtration [65], wet spinning [66], the coating method [67,68],

the in situ growth method [69], and atomic layer deposition [70] are more commonly used to prepare separators.

3.1. Electrospinning

Electrospinning is a novel technique for preparing nanofiber separators, the principle of which is as follows: under the action of a high-voltage electrostatic field, the polymer forms a Taylor cone when it flows out of the needle, and a continuously charged jet is ejected and deposited on the collector as nonwoven nanofibers [71]. The nanofibers prepared by electrospinning can reach the nanometer diameter [64,72], and the prepared nanofiber separator has the advantages of high porosity, large specific surface area, and small pore size [73]. As shown in Figure 5, electrospinning technology has prepared a variety of nanostructured fibers. The electrospinning method has received great attention in the field of battery separators in recent years.

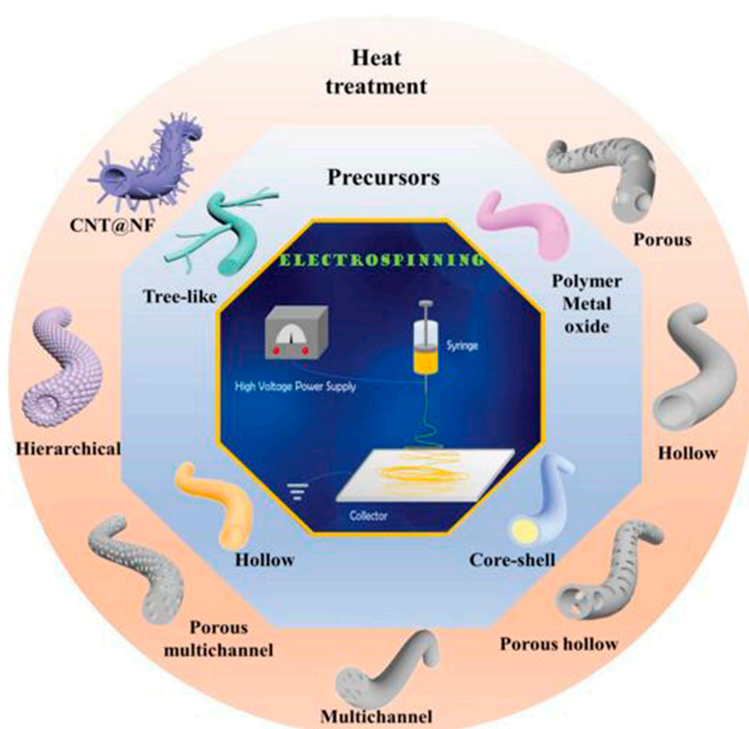


Figure 5. The electrospinning technology has prepared a variety of nanostructured fibers [2]. Reproduced with permission from the Advanced Functional Materials.

3.2. Vacuum Filtration

The vacuum filtration method is a new method for preparing separators using the interfacial composite method, which has the advantages of convenient operation, a simple process, and no specific process equipment. Its working principle is that the film-forming material is uniformly dispersed in the solvent, and then under vacuum filtration conditions, the film-forming material is deposited on the substrate due to the flow function of solvent molecules. The disadvantage is that due to the limitations of process conditions, the structure of the produced nanofibers is uncontrollable and unsuitable for large-scale mass production [74].

3.3. Wet Spinning

The nanofiber non-woven separator prepared by the wet laying method has high porosity and good affinity with electrolytes [75]. The principle is that different polymer fibers are used to separate matrix fibers and adhesive fibers, which are continuously randomly laid on the screen belt after mixing in a water-soluble suspension, sent to a

ventilation drying box to heat and soften the bonded fibers, and then calendered by a heating drum to obtain a non-woven film [62]. The disadvantages are that the structure and properties of the nanofibers prepared by this method are limited by the type and composition of the polymer in the suspension, and the operation is more complicated [76].

3.4. Coating Method

The coating method is one of the most commonly used modification methods. A layer of modified material is coated on one side of the separator by means of physical methods, and polysulfides are adsorbed by the modified material to improve the shortcomings of the separator. Because the coating method is simple to operate, relatively low in cost, can be used for large-area separator modification, and is suitable for industrial production, the coating method is widely used in the modification of lithium–sulfur battery separators. However, the coating method has problems such as difficulty in accurately controlling the thickness of the separator. The viscosity of the material has an impact on the coating effect, and some polymer materials are not suitable for the preparation of the coating method.

3.5. In Situ Growth Method

The in situ growth method is a relatively novel method of separator modification. Compared with other modification methods, this method can effectively generate a lightweight barrier on one side of the separator and avoid excessive thickness of the separator; in addition, the in situ growth method can achieve efficient use of materials, thereby reducing costs. However, the current in situ growth method is still in the experimental research stage. In addition, the modification process is relatively complicated, and it is difficult to achieve mass production.

3.6. Atomic Layer Deposition (ALD)

Atomic layer deposition is a method in which substances can be plated on the surface of the substrate, layer by layer, in the form of a single-atom film. It has similarities to chemical vapor deposition [77]. Its working principle is a method in which a gas precursor pulse alternately enters the reactor and chemically adsorbs and reacts on the deposition matrix to form a deposition film. A typical ALD cycle consists of two self-limiting semi-reactions [78], and it is this reaction property that allows the separator's thickness to be precisely controlled. However, the atomic layer deposition method has disadvantages such as high requirements for reaction conditions, a complicated production process, expensive equipment, and a slow deposition rate.

4. Application of Separators in Lithium–Sulfur Batteries

As is evident from the preceding discussion, the separator plays a crucial role in influencing the electrochemical performance of lithium–sulfur batteries. In the subsequent section, we will delve into the utilization of separators fabricated through various methods within the context of lithium–sulfur batteries. The interlayer, being an integral component of the separator, typically resides between the positive electrode and the separator. Its exceptional attributes, such as the heightened surface area and excellent electronic conductivity, facilitate the diffusion of lithium ions and the conduction of electrons. Moreover, we will expound upon the application of interlayers prepared via different techniques in lithium–sulfur batteries.

4.1. Electrospinning

4.1.1. Separator

In Li-S, the separator is required to suppress the shuttle effect, good electrolyte wettability, and good ionic conductivity [79]. Nanofiber separators prepared using the electrospinning technique exhibit extremely fine fibers, with exceptionally high specific surface areas. Additionally, these separators possess a notably high level of porosity, a feature inherent to their unique fabrication process. Owing to their elevated specific surface areas and

porosity, such separators can provide a greater quantity of electrolytes during the charge and discharge processes of lithium–sulfur batteries. This augmentation of reaction sites enhances electrochemical reactions. In recent years, numerous researchers have achieved significant advancements by incorporating modified materials onto the fiber surface, aiming to adsorb polysulfides and mitigate the shuttle effect, thereby improving the cyclic lifespan and practical specific capacity of the batteries (Guo et al. [80]). A PAN film doped with Al_2O_3 particles was prepared using the electrospinning method and studied as a separator for Li-S. Figure 6 shows the preparation process of the separator and the excellent electrochemical performance of the lithium–sulfur battery using the separator. It can be seen from the figure that Al_2O_3 particles attached to the PAN nanofibers, and the separator exhibited strong chemical interaction, which blocked polysulfides from passing through the separator and inhibited the shuttle effect. The PAN/ Al_2O_3 separator was thermally stable at 200 °C. The lithium–sulfur battery with this separator exhibited low resistivity ($R_{\text{SEI}} = 14.25 \Omega$, $R_{\text{CT}} = 7.32 \Omega$). Under a 200 mA/g constant current charge and discharge, the remaining capacity after 100 cycles was 639 mAh/g (compared with pure PAN and PP separator batteries, which achieved only 380 mAh/g and 233 mAh/g), and the Coulombic efficiency was 99.76%.

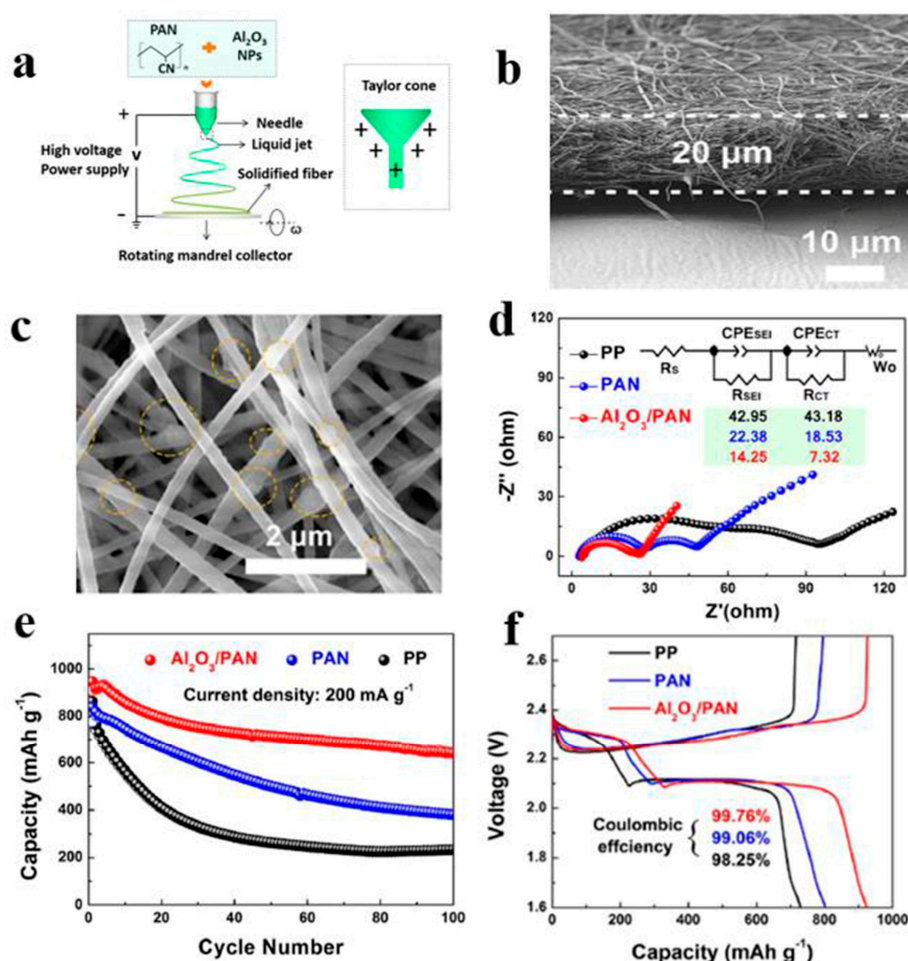


Figure 6. Application of an electrospinning separator in lithium–sulfur batteries: (a) Preparation process. (b) Cross–sectional morphologies of $\text{Al}_2\text{O}_3/\text{PAN}$ separator prepared by electrospinning. (c) The SEM image shows Al_2O_3 distributed on the fiber. (d) EIS curve. (e) Cycle curve. (f) Charge–discharge curve [80]. Reproduced with permission from the *Electrochimica Acta*.

In comparison to traditional PP separator separators, electrospun nanofiber separators have garnered considerable attention due to their exceptional specific surface areas

and extensive porosity. They exhibit unparalleled advantages in terms of electrolyte absorption and ion transport, positioning them as a focal point in research for potential battery separators.

4.1.2. Interlayer

A highly conductive electrospun nanofiber interlayer is introduced between the positive electrode and the separator to effectively improve the performance of lithium–sulfur batteries. Electrospun carbon nanofibers, owing to their excellent electrical conductivity, serve to reduce internal resistance within batteries, thus enhancing the rates of electron and ion transport. Additionally, carbon nanofibers exhibit Van Der Waals interactions with polysulfides, facilitating their adsorption. Guo et al. [81]. utilized electrospinning technology to prepare a $\text{Ti}_4\text{O}_7/\text{C}$ nanofiber (TCNF) interlayer. The incorporation of carbon nanofibers in this interlayer offered several advantages, including a large specific surface area and high electrical conductivity, which significantly enhanced the conversion and electron transfer of polysulfides. Additionally, Ti_4O_7 formed strong chemical bonds with polysulfides, effectively mitigating their shuttle effect. Figure 7 illustrates the separator preparation process and demonstrates the exceptional electrochemical performance of the lithium–sulfur battery utilizing this separator. TEM and SEM images reveal the random distribution of Ti_4O_7 particles on the fiber's surface, leading to substantial inhibition of polysulfide shuttling and a notable improvement in the electrochemical performance of lithium–sulfur batteries. At a discharge rate of 0.2 C, the initial specific capacity reached an impressive 1304 mAh g^{-1} , with the capacity maintained at 945 mAh g^{-1} after 100 cycles. During high-rate cycling tests at 5 C, the initial specific capacity was 610 mAh g^{-1} , and even after 300 cycles, the capacity remained at approximately 400 mAh g^{-1} , with a minimal capacity decay of only 0.11% per cycle. Furthermore, in the impedance diagram, the TCNFs interlayer exhibited the lowest AC impedance, measuring only 40Ω (that of the comparison sample was 138Ω).

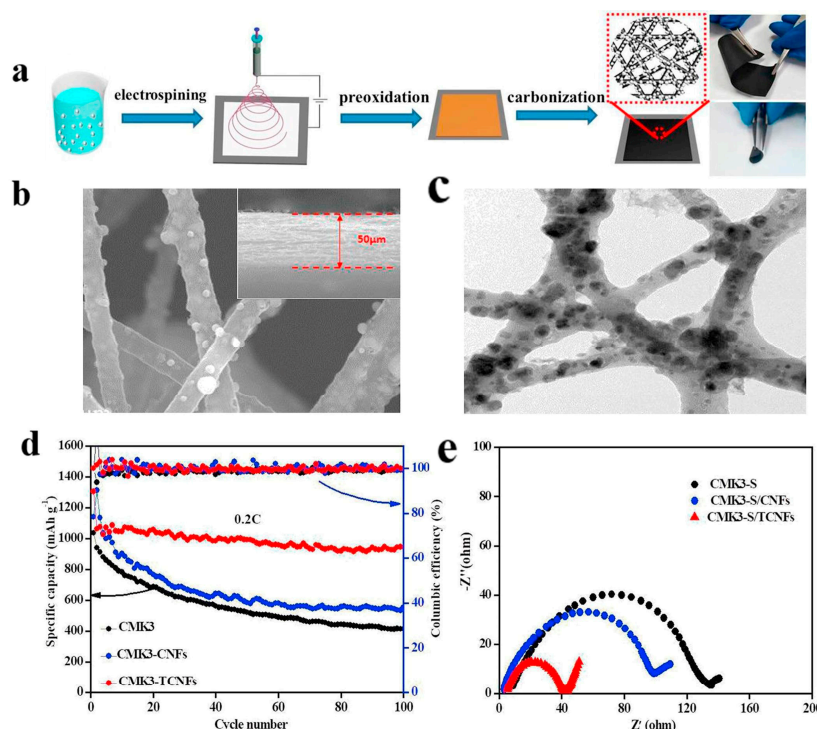
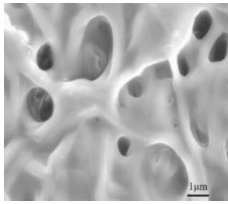
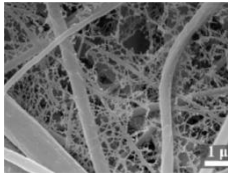
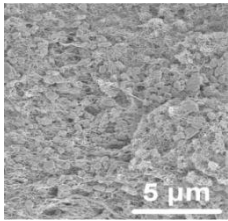
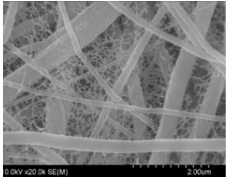
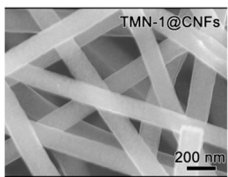
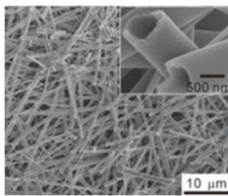
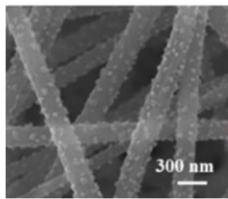


Figure 7. Application of electrospinning interlayer in lithium–sulfur batteries: (a) interlayer preparation process; (b) SEM images of TCNFs; (c) TEM images of TCNFs; (d) cycling stability of CMK3–S, CMK3-S/CNFs, and CMK3-S/TCNFs interlayers at 0.2 C for 100 cycles; (e) EIS curve [81]. Reproduced with permission from the Chemical Engineering Journal.

Introducing an electrospun nanofiber interlayer with high electrical conductivity and surface area between the positive electrode and separator serves not only to enhance the conductivity of the integrated electrode, but also to significantly suppress the migration of polysulfides towards the negative electrode side. As shown in Table 1, the application of electrospinning separators and interlayers in lithium–sulfur batteries is demonstrated.

Table 1. Applications of electrospun separators and interlayers in lithium–sulfur batteries.

	Main Materials	Initial Capacity (mAh g ⁻¹)	Capacity Remaining (mAh g ⁻¹)	Decay Rate	SEM Figure	Reference
Separator	PVDF/PSSLi	955	466 (0.5 C, 200 cycles)	0.26%		[82]
	PVDF/MOF	1324.2	551 (2 C, 700 cycles)	0.05%		[83]
	PI/MC	1602.3	905.5 (0.2 C, 100 cycles)	---		[84]
	PMIA	1222.25	745.7 (0.5 C, 800 cycles)	---		[85]
Interlayer	TMN@CNF	947	390 (2 C, 1000 cycles)	0.059%		[86]
	TCNF	1279	798 (2.5 A g ⁻¹ , 1000 cycles)	0.057%		[87]
	CoSe@NC	1317	804.7 (0.1 C, 100 cycles)	---		[88]

4.2. Vacuum Filtration

4.2.1. Separator

According to Yigeng et al. [89], They modified the PP separator through suction filtration, a depositing a layer of g-C₃N₄ composite on one side of it. It had abundant adsorption sites and contributed to the solidification of polysulfides. The process of polysulfide solidification entails immobilizing polysulfide species onto the cathode material or the cathode-proximate regions of the separator. This strategic immobilization serves as an effective countermeasure against the undesirable migration of polysulfides towards the anode, thereby mitigating capacity fade and consequentially augmenting the performance characteristics of lithium–sulfur batteries. As shown in Figure 8, the schematic diagram of the suction filter system is shown, and SEM revealed that the PP separator has large pores, that polysulfides are easy to pass through, and that the modified g-C₃N₄ separator could not see the large pores of PP. Through electrochemical impedance analysis (EIS), after cycling, it was seen that the modified g-C₃N₄ separator had a small impedance. When the discharge current was restored to 0.2 C, the reversible capacity could be restored to 830 mAh g⁻¹, indicating that the electrochemical stability of the separator after modification had been significantly enhanced. It can be seen from the cycle performance chart that at 0.2 C, the initial discharge-specific capacity was 990 mAh g⁻¹; after 200 cycles, the discharge-specific capacity was 829 mAh g⁻¹, and the capacity retention rate was 83.7%.

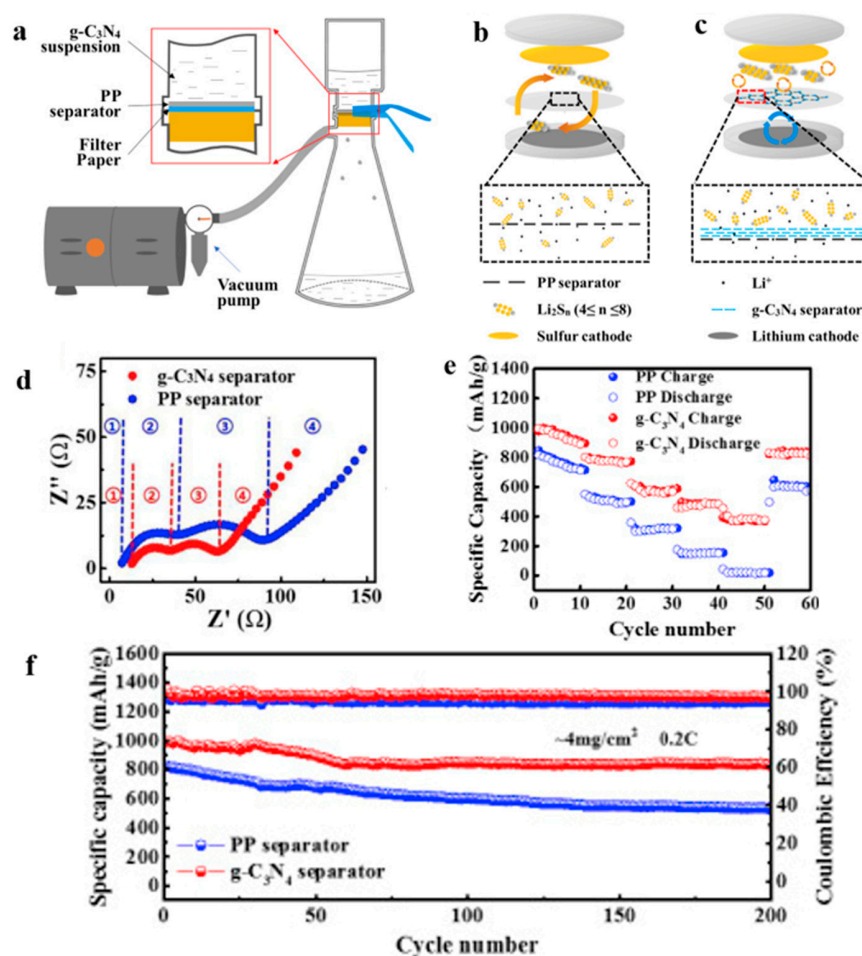


Figure 8. Application of a separator prepared by vacuum filtration method in a lithium–sulfur battery: (a) Schematic diagram of separator modification, (b) schematic diagram of PP separator barrier to polysulfide, (c), schematic diagram of g-C₃N₄/PP separator barrier to polysulfide, (d) Electrochemical impedance spectroscopy after cycling, (e) rate performance, and (f) cycle curve [89]. Reproduced with permission from the *Electrochimica Acta*.

The vacuum filtration method provides the advantages of high porosity, consistency, controllability, and cost-effectiveness for the preparation of lithium–sulfur battery separators.

4.2.2. Interlayer

Feng et al. [90] prepared a 2D NiCo MOF/CNT as the middle layer of a lithium–sulfur battery and filtered it onto PP through vacuum filtration. As shown in Figure 9, the thickness of 2D NiCo MOF/CNT was only a few nanometers, and the CNT built a conductive network to enhance electronic conductivity while serving as a physical barrier to prevent polysulfide migration. The 2D NiCo MOF/CNT improved the catalytic performance due to abundant and accessible active sites. The lithium–sulfur battery using 2D NiCo MOF/CNT interlayer had an initial discharge-specific capacity of $1132.7 \text{ mAh g}^{-1}$ at 0.5 C , and it maintained 709.1 mAh/g^{-1} after 300 cycles, showing good cycle stability and rate performance.

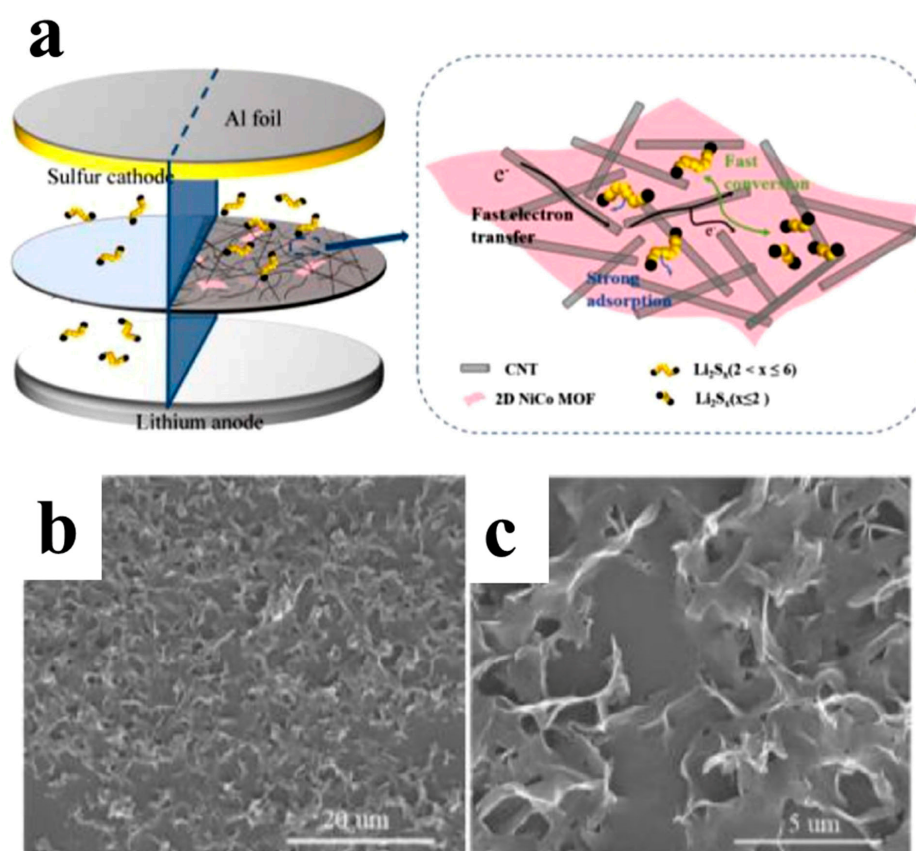
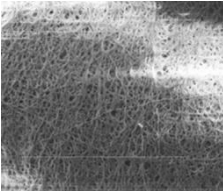
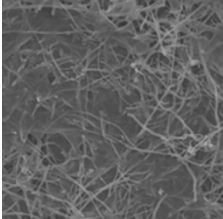
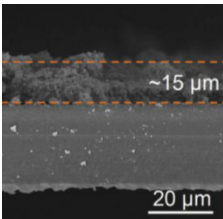
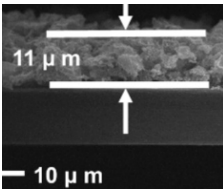
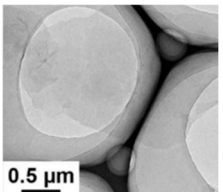
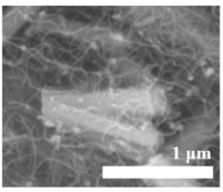


Figure 9. Application of interlayer prepared by vacuum filtration method in a lithium–sulfur battery: (a) Internal diagram of the battery, (b,c) SEM at different magnifications [90]. Reproduced with permission from the Chinese Chemical Letters.

Whether for the preparation of separators or interlayers, using vacuum filtration provides the advantages of high porosity, consistency, controllability, and cost-effectiveness. Shown in Table 2 is the application of the separator and interlayer prepared by the vacuum filtration method in lithium–sulfur batteries.

Table 2. Applications of vacuum filtration separators and interlayers in lithium–sulfur batteries.

Main Materials	Initial Capacity (mAh g ⁻¹)	Capacity Remaining (mAh g ⁻¹)	Decay Rate	SEM Figure	Reference	
Separator	BC	1175	735 (0.3 C, 300 cycles)	0.07%		[91]
	HCNF/rGO	1318.4	533.6 (1 C, 400 cycles)	0.13%		[92]
	CF/PP	1111	683 (0.5 C, 500 cycles)	0.071%		[93]
	NiFe ₂ O ₄ -NiO/PP	1350	755 (2 C, 1000 cycles)	0.065%		[94]
Interlayer	MOF	850	604 (1 C, 900 cycles)	0.032%		[95]
	Co-MOF-74@MWCNT	1434	771 (0.1 C, 200 cycles)	---		[96]

4.3. Wet Spinning

Currently, commercial PP and PE separators are prepared using a wet process. However, when used directly in lithium–sulfur batteries, the PP separator leads to a significant shuttle effect, resulting in a sharp decrease in the specific discharge capacity of the battery. Therefore, we will not elaborate on the application of PP separators in lithium–sulfur batteries separately in this context. Main applications include functional interlayers in Li-S [18,97–100] and electrodes [101,102]. Li et al. [98] successfully prepared a carbon paper sandwich via a wet process with excellent electrical conductivity of 11.9 S cm⁻¹. A high initial capacity, up to 1091 mAh g⁻¹, was achieved when using carbon paper as an interlayer for Li-S. At 5 C, 631 mAh g⁻¹ was maintained after 200 cycles (0.21% capacity decay

per cycle). Zhang et al. [103], prepared the PMB-SNWs interlayer through a wet process. The interlayer was applied in lithium–sulfur batteries and exhibited good electrochemical performance. At 2 C, the initial discharge-specific capacity was 877 mAh g^{-1} ; it maintained 782 mAh g^{-1} after 850 cycles, and the decay rate per cycle was as low as 0.013%.

4.4. Coating Method

4.4.1. Separator

Polar metal oxide titanium dioxide (TiO_2) exhibits a strong chemical interaction with polysulfides, making it widely applicable in the field of lithium–sulfur batteries. This is attributed to the ability of oxygen atoms on the surface of TiO_2 to form chemical bonds with sulfur atoms present in polysulfides, facilitating the effective adsorption of polysulfides. Additionally, the high electronegativity of the TiO_2 surface enables it to counteract the shuttle effect of polysulfides through a charge repulsion mechanism. Gao et al. [57] coated the PP separator with a layer of titanium dioxide, modified multi-walled carbon nanotube composites ($\text{TiO}_2@\text{SCNT}/\text{PP}$ separator), and applied the separator to Li-S, and the data showed that the performance of the separator and the pre-modification period greatly improved. In Figure 10, the battery's schematic diagram and the SEM images illustrate the separator preparation process for blocking polysulfides. The SCNTs are intertwined to form a conductive framework that enhances electron transport. TiO_2 particles are embedded in SCNT, and have a strong chemical adsorption effect which can inhibit the shuttle effect. By comparing the color changes of polysulfides, it was also shown that the PP separator coated with $\text{TiO}_2@\text{SCNT}$ composites had a good adsorption effect on polysulfides. Electrochemical performance is an important measure of the battery, and this separator was assembled in the battery. The data show that the performance was best when the coating thickness was 200, denoted as $\text{TiO}_2@\text{SCNT-200}/\text{PP}$, at 0.5 C. The initial discharge specific capacity of the composite separator was $1103.9 \text{ mAh g}^{-1}$ (compared to PP separator 218.5 mAh g^{-1}); after 200 cycles, the capacity ratio was 848.0 mAh g^{-1} (compared to PP separator is 172.2 mAh g^{-1}); and after 900 cycles, it maintained 446.8 mAh g^{-1} . The capacity decay per cycle was only 0.066%. The electrochemical performance was greatly improved compared to the PP separator.

4.4.2. Interlayer

Wang et al. [104] prepared the NC-Co interlayer using a coating method. The intermediate layer effectively inhibited the shuttling of polysulfides. As shown in Figure 11, at 1 C, the first discharge-specific capacity of the lithium–sulfur battery using the interlayer was $1216.9 \text{ mAh g}^{-1}$, and it maintained 660.3 mAh g^{-1} after 250 cycles. The Coulombic efficiency remained above 99% during the cycle. After 100 cycles, the surface SEM of the negative lithium metal showed that the lithium negative electrode with the interlayer had few surface cracks, while the lithium metal without the interlayer had obvious cracks, indicating that the use of the interlayer can significantly inhibit the corrosion of the negative metal lithium.

The coating method can provide structural uniformity, controllability, multiple material options, and cost-effectiveness. These characteristics are very beneficial for the preparation of lithium–sulfur battery separators and interlayers. Shown in Table 3 is the application of separators and interlayers prepared using the coating method in lithium–sulfur batteries.

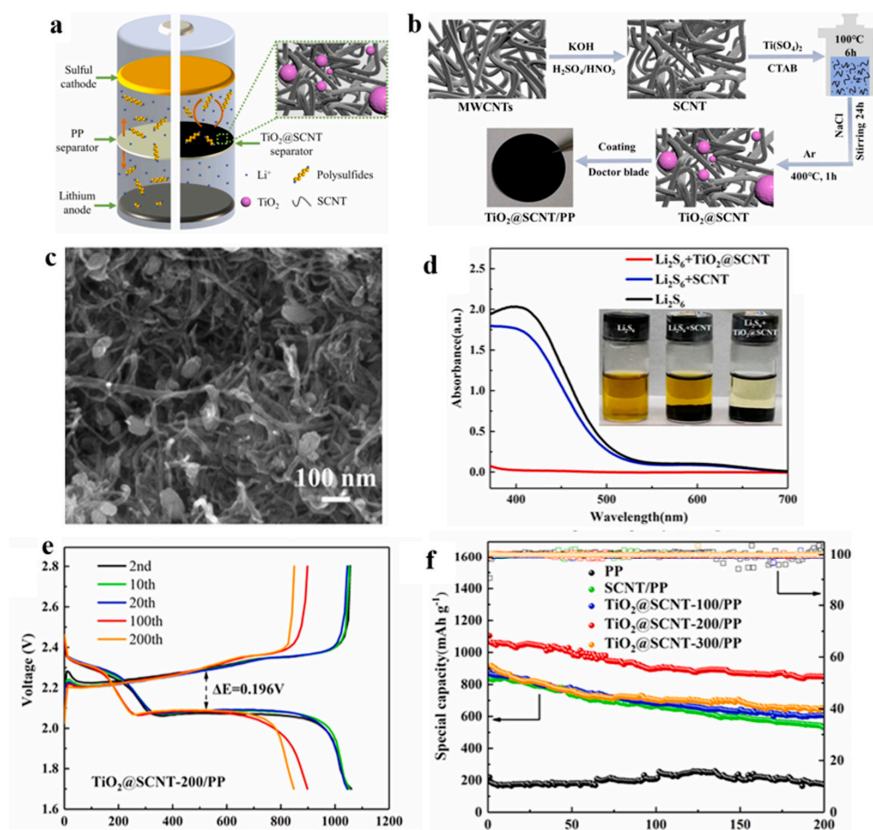


Figure 10. Application of a separator prepared by the coating method in lithium–sulfur batteries: (a) schematic diagram of the battery, (b) preparation flow chart, (c) scanning electron microscopy diagram, (d) schematic diagram of the adsorption effect of polysulfide, (e) charge and discharge curve, and (f) After 200 cycles at 0.5C [57]. Reproduced with permission from the Journal of Alloys and Compounds.

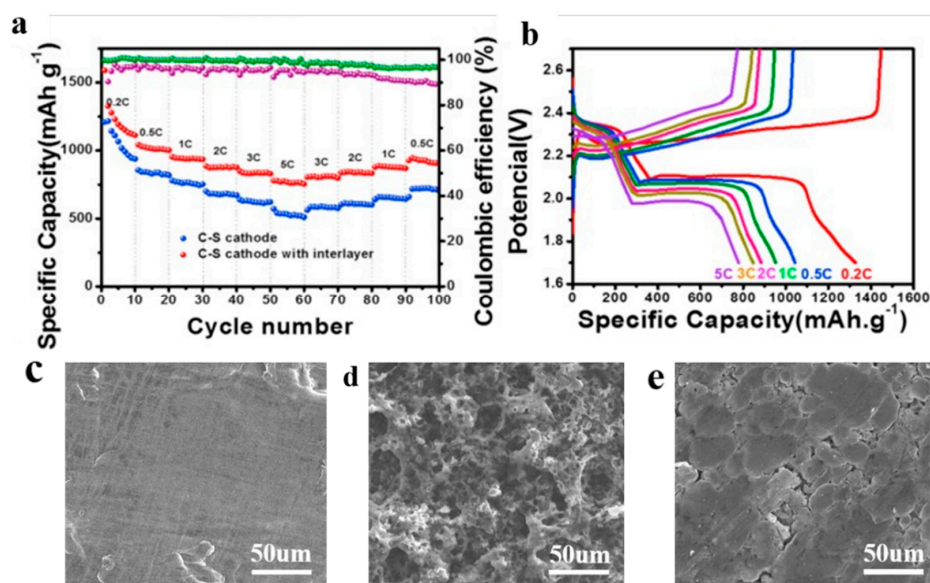
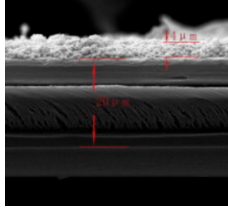
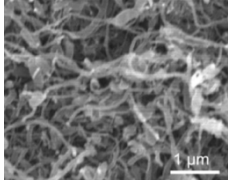
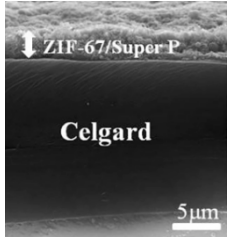
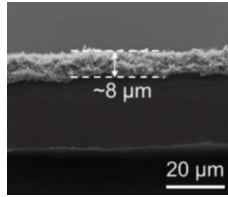
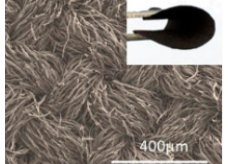
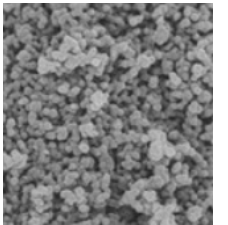


Figure 11. Application of an interlayer prepared by the coating method in lithium–sulfur batteries: (a) differences in specific capacity and Coulomb efficiency at various rates, (b) its corresponding voltage–capacity profiles at various rates, (c) lithium metal surface before cycling, (d) lithium metal surface after cycling without interlayer, (e) lithium metal surface after cycling with interlayer [104]. Reproduced with permission from the Chemical Engineering Journal.

Table 3. Applications of separators and interlayers prepared using the coating method in lithium–sulfur batteries.

	Main Materials	Initial Capacity (mAh g ⁻¹)	Capacity Remaining (mAh g ⁻¹)	Decay Rate	SEM Figure	Reference
Separator	Al ₂ O ₃ /PP	967	593.4 (0.5 C, 50 cycles)	0.13%		[105]
	Zr-MOF@CNT/PP	1157	545 (1 C, 500 cycles)	0.067%		[106]
	ZIF-67/PP	1341	761 (0.2 C, 300 cycles)	0.14%		[107]
	RP/PP	1287	729.6 (1 C, 500 cycles)	0.109%		[108]
Interlayer	CFF	1346.9	1076.6 (0.1 C, 100 cycles)	---		[109]
	OMNC	994.4	587.6 (0.5 C, 100 cycles)	---		[110]

4.5. In Situ Growth Method

4.5.1. Separator

Lu et al. [111] modified a PP separator via in situ growth. On the side of the PP separator, a layer of polar hydrated sulfate CoSO₄·4H₂O material (CS/PP separator) was grown in situ, and the cobalt sulfate hydrate had strong polarity and catalytic properties, which can effectively adsorb polysulfides. As shown in Figure 12, in the preparation flow chart, it can be seen by scanning electron microscopy that the surface of the separator was attached to a layer similar to the shape of a sea urchin, the single sea urchin was assembled from the nanoneedles of several microns, and the separator exhibited good mechanical

stability. The data show that when the material reaction time was 6 h, the separator showed the best performance, which was denoted as CS/PP-6. At 1 C, the initial specific capacity of the modified separator reached as high as 807.7 mAh g^{-1} . After 500 cycles, it still maintained 504.6 mAh g^{-1} (compared to 208.7 mAh g^{-1} for the PP separator), and the Coulombic efficiency reached as high as 97%. When the discharge current was restored to 0.1 C, the reversible capacity was $1308.6 \text{ mAh g}^{-1}$, indicating that the lithium–sulfur battery using the separator had good reversibility and good electrochemical performance.

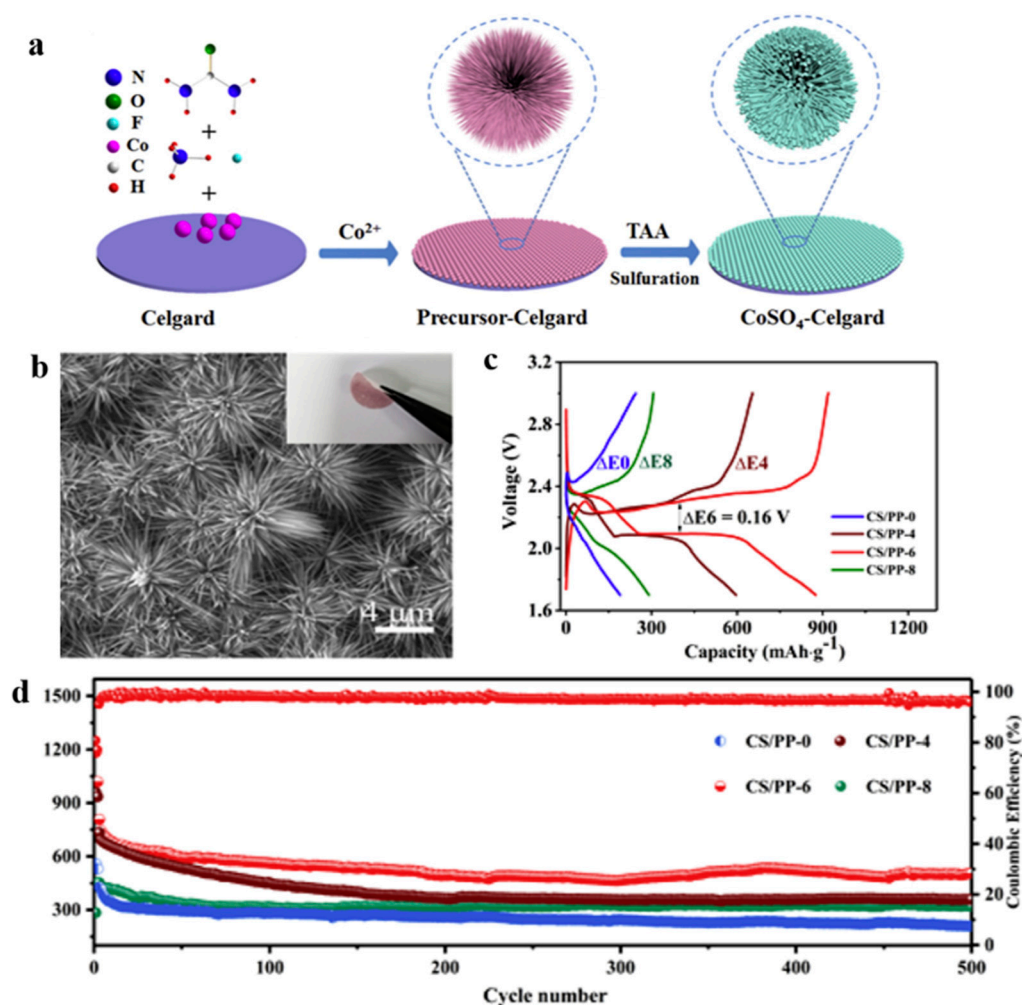


Figure 12. Application of a separator prepared using the original growth method in lithium–sulfur batteries: (a) preparation flow chart, (b) scanning electron microscopy diagram, (c) charge and discharge curve, and (d) cycle curve [111]. Reproduced with permission from the Journal of Alloys and Compounds.

4.5.2. Interlayer

Li et al. [112] prepared the ZIF/CNFs interlayer via the situ growth method. As shown in Figure 13, the interlayer had an obvious effect of inhibiting polysulfide shuttling. According to SEM and TEM images, ZIF-64 particles were distributed on the fiber, and due to the special binding site of ZIF-64, it inhibited the shuttling of polysulfides during circulation. At 1 C, it exhibited a high discharge-specific capacity of 1334 mAh/g , which remained at 569 mAh/g after 300 cycles.

The in-situ growth method has high controllability and nanoscale pore structure in the preparation of lithium–sulfur battery separators and interlayers, which can significantly improve battery performance. As shown in Table 4, the application of separators and interlayers prepared by the situ growth method in lithium–sulfur batteries.

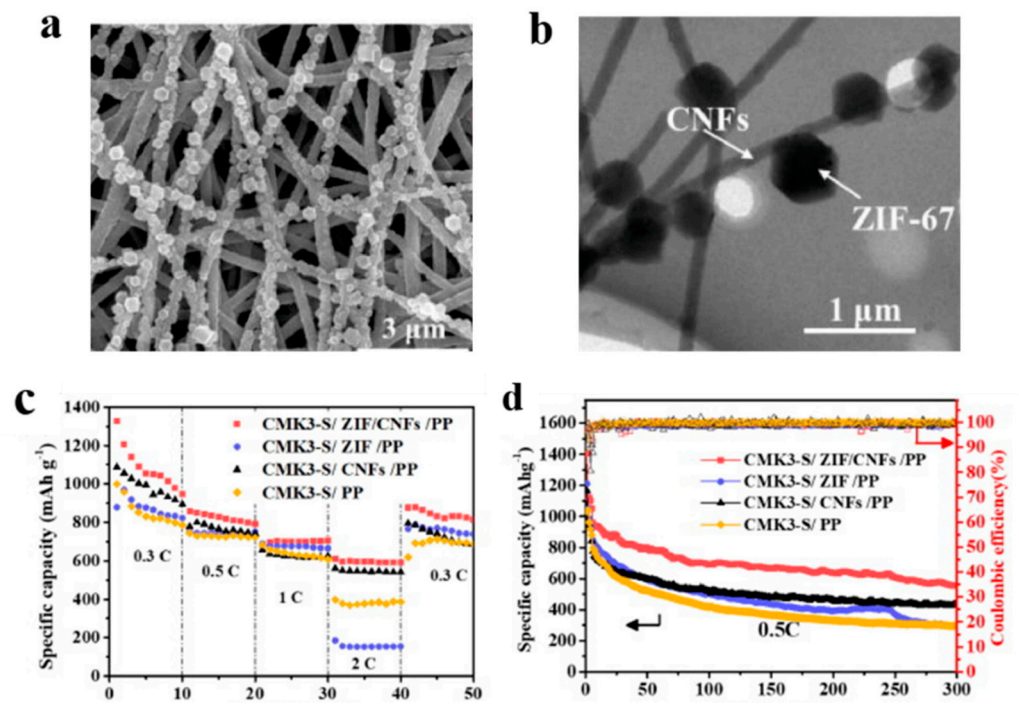
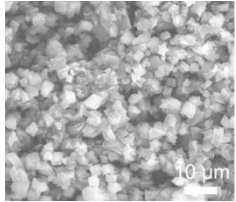
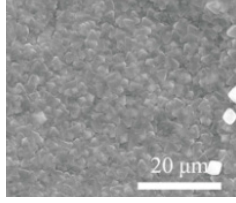


Figure 13. Application of Interlayer Prepared by Original Growth Method in Lithium-sulfur Batteries: (a) SEM image of ZIF/CNFs, (b) TEM image of ZIF/CNFs, (c) Rate performance, (d) After 300 cycles at 0.5C [112]. Reproduced with permission from the Journal of Energy Chemistry.

Table 4. Applications of the situ growth method separators and interlayers in lithium-sulfur batteries.

Main Materials	Initial Capacity (mAh g ⁻¹)	Capacity Remaining (mAh g ⁻¹)	Decay Rate	SEM Figure	Reference	
TA-Co/PP	1182	549.9 (2 C, 500 cycles)	0.065%		[69]	
Separator	Z-PMIA	1391.2	961.1 (0.2 C, 350 cycles)	0.033%		[55]
	PMIA/ZIF-8	1156	855 (0.2 C, 300 cycles)	0.086%		[113]

Table 4. Cont.

Main Materials	Initial Capacity (mAh g ⁻¹)	Capacity Remaining (mAh g ⁻¹)	Decay Rate	SEM Figure	Reference	
Interlayer	MIL-101/CNT	816	628 (1 C, 500 cycles)	0.046%		[114]
	MOF-808	908.1	755.5 (1 C, 500 cycle)	0.03%		[115]

4.6. Atomic Layer Deposition

4.6.1. Separator

At present, owing to the distinctive attributes of the Atomic Layer Deposition (ALD) fabrication process, there is a scarcity of literature that directly employs ALD for the modification of polypropylene (PP) separators. Usually, people use methods such as cooperating with other preparation processes (coating, suction filtration, etc.) to modify the separator. Details are shown in Section 4.7.1.

4.6.2. Interlayer

Lin et al. [70]. prepared the CNT@SACo interlayer by atomic layer deposition and applied it to lithium–sulfur batteries. Figure 14 shows the preparation process flow chart. From the experimental results, the CNT@SACo interlayer exhibits catalytic activity catalyzes the conversion of polysulfides, and inhibits the shuttling of polysulfides. The lithium–sulfur battery with the CNT@SACo interlayer exhibited a high discharge specific capacity of 880 mAh/g at 1 C, and maintained a capacity of 595 mAh/g after 500 cycles, with a capacity decay rate of 0.064% per cycle.

The Atomic Layer Deposition method has highly precise film control and uniform material distribution in the preparation of the middle layer of lithium–sulfur batteries, which helps improve battery performance. As shown in Table 5, the application of interlayers prepared by Atomic Layer Deposition (ALD) in lithium–sulfur batteries.

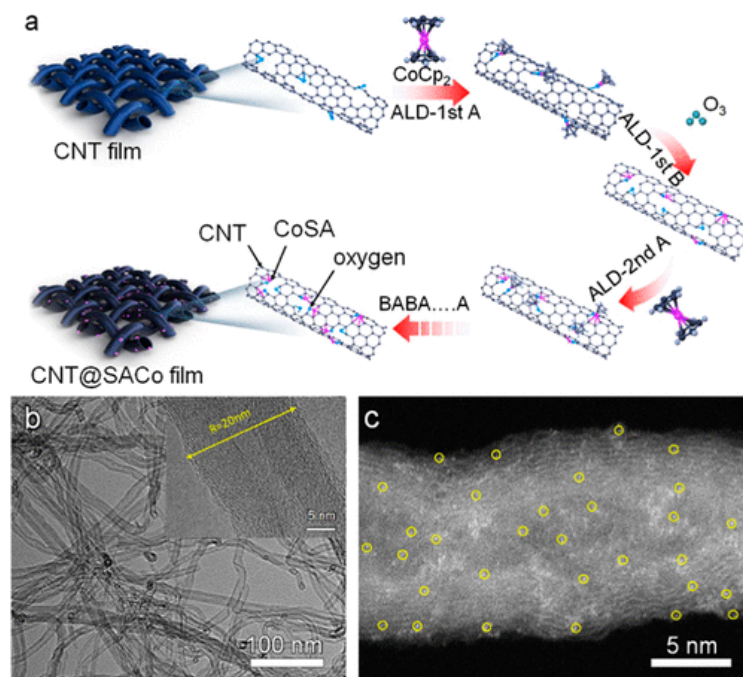
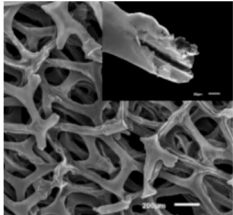
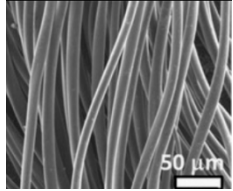
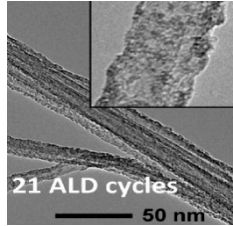


Figure 14. Application of Interlayer Prepared by Atomic Layer Deposition in Lithium–sulfur Batteries: (a) Schematic illustration of the preparation process of the CNT@SACo interlayer by the ALD method, (b) TEM of CNT@SACo, (c) high-angle annular dark-field scanning transmission electron microscopy (HAADF-STEM) image of CNT@SACo [70]. Reproduced with permission from the ACS Applied Energy Materials.

Table 5. Applications of Atomic layer deposition (ALD) separators and interlayers in lithium–sulfur batteries.

Main Materials	Initial Capacity (mAh g ⁻¹)	Capacity Remaining (mAh g ⁻¹)	Decay Rate	SEM Figure	Reference
ALD-ZnO	998	846 (0.2 C, 100 cycles)	---		[116]
Interlayer Al ₂ O ₃	1136	766 (40 cycles)	---		[117]
HfO ₂ -CNT	1275	995 (0.2 C, 100 cycles)	---		[118]

4.7. Composite Process

4.7.1. Separator

Ding et al. [119] prepared multi-walled carbon nanotubes @titanium dioxide quantum dots (MWCNTs@TiO₂) modified PP separators using atomic layer deposition (ALD). Figure 15 shows a flow chart of the preparation process. It can be seen from scanning electron microscopy that the initial PP separator had a large pore size, and the MWCNTs@TiO₂ was intertwined after modification. The porosity increased and the pore size was improved, effectively preventing soluble polysulfides from shuttling into the anode through the separator. The electrochemical data of the cell showed that the Coulombic efficiency and cycle stability of Li-S cells were improved. At 0.5 C, the capacity decay of Li-S using this separator was reduced to 0.072% per cycle.

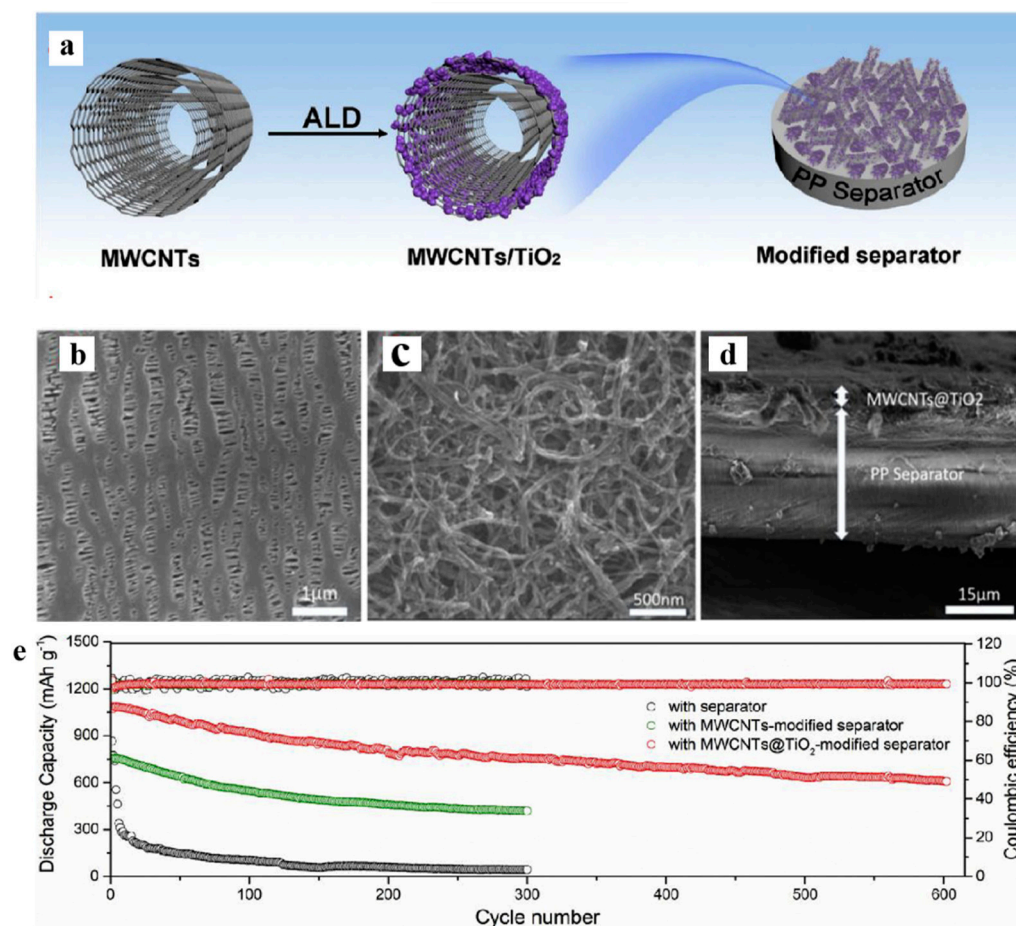


Figure 15. Application of a separator prepared by the composite process in lithium–sulfur batteries: (a) schematic diagram of preparation, (b) PP separator SEM, (c) MWCNTs@TiO₂/PP separator SEM, (d) MWCNTs@TiO₂/PP separator profile SEM, and (e) cycle curve [119]. Reproduced with permission from the *Electrochimica Acta*.

4.7.2. Interlayer

Sang-Hyun Moon et al. [120] used a combination of electrospinning and vacuum filtration to prepare a 1T-MoS₂/CNF intermediate layer and applied it to lithium–sulfur batteries. As shown in Figure 16, carbon nanofibers have strong conductivity and can effectively reduce interface resistance. MoS₂ can strongly adsorb the Li₂S_x due to interactions of S-S and metal-S bonds, preventing the dissolution of Li-polysulfide in a liquid electrolyte. When the interlayer is applied to lithium–sulfur batteries, it exhibits good electrochemical performance. After 500 cycles at 1 C, the capacity retention rate was 73% under 1C. The initial specific capacity reached as high as 480 mAh g⁻¹.

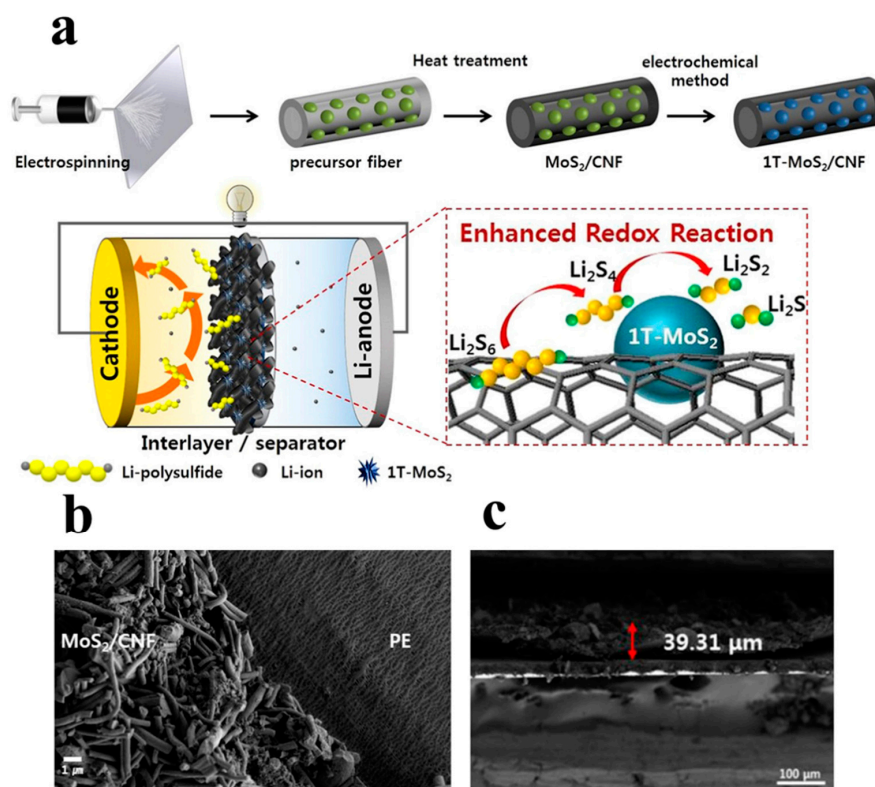


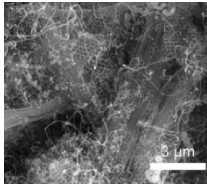
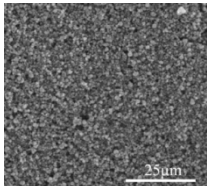
Figure 16. Application of an interlayer prepared using the composite process in lithium–sulfur batteries: (a) schematic diagram of preparation, (b) SEM, (c) TEM [120]. Reproduced with permission from the Journal of Alloys and Compounds.

Shown in Table 6 is the application of interlayers prepared by the composite process in lithium–sulfur batteries.

Table 6. Applications of composite process separators and interlayers in lithium–sulfur batteries.

Main Materials	Initial Capacity (mAh g ⁻¹)	Capacity Remaining (mAh g ⁻¹)	Decay Rate	SEM Figure	Reference
Ni-Co MOF@PAN	944	794 (2 C, 2000 cycles)	0.034%		[121]
Separator PAN/PDAAQ	881	766 (1 C, 800 cycles)	0.11%		[122]
UIO66@BP/PAN	---	761 (0.5 C, 1000 cycles)	0.016%		[123]

Table 6. Cont.

Main Materials	Initial Capacity (mAh g ⁻¹)	Capacity Remaining (mAh g ⁻¹)	Decay Rate	SEM Figure	Reference	
Interlayer	N _x /Co-TiO ₂ /NCNT@CNFs	1132	988 (0.2 C, 100 cycles)	---		[124]
	CNF@VS 2/CNT	834	605 (1 C, 1145 cycles)	---		[125]

5. Conclusions and Outlook

In recent years, with the rising demand for new energy, it has become important to develop an energy storage system with high energy density, low cost, and a long cycle life. Traditional lithium batteries have a high cost and low energy density, which makes it difficult for them to meet the huge market demand. Li-S batteries are regarded as one of the most promising energy storage systems due to their high theoretical specific capacity and low cost. Li-S batteries also have some urgent problems to solve, such as poor conductivity of S, the expansion of the positive electrode volume during the electrochemical reaction, and the most important problem, the shuttle effect caused by polysulfides. As an important component of lithium–sulfur batteries, separators are very important in suppressing the shuttle effect of polysulfides.

From the perspective of separator preparation, the research mainly focuses on the preparation of new separator materials and the modification of traditional separators. Due to their high porosity and liquid absorption rates, electrospinning technology can effectively enhance the actual discharge-specific capacity of lithium–sulfur batteries. However, the electrospun fiber separator tends to have a relatively large thickness and low mechanical strength. In this field, future advancements can be made by starting at the raw material level to develop high-performance electrospun nanofibers that exhibit excellent strength and temperature resistance. For instance, the PI fiber demonstrates exceptional temperature resistance, along with favorable mechanical properties and other new electrospinning separation materials, including PAN, polyvinyl chloride (PVC), PVDF, and polyethylene oxide (PEO) separators.

Lithium–sulfur batteries have undergone significant progress; however, most research is still based on cylindrical cell designs. The real operational environment for pouch-type cells is more demanding due to their lower sulfur active material content, making it challenging to achieve high energy density. Additionally, the fabrication processes for modified separators and interlayers are currently not scalable and come with higher costs. Through the optimization of separator structures and the exploration of new materials, there is potential to further enhance the electrochemical performance of lithium–sulfur batteries while reducing the costs. Some perspectives regarding the future of lithium–sulfur battery separators in terms of structural design and material selection are listed as follows: (1) ion-selective separators: This type of separator can block the shuttling of polysulfides while allowing for the passage of lithium ions. Implementing ion-selective separators holds the promise of improving Coulombic efficiency and battery cycle life. (2) Multilayer structure separators: Multilayer separators composed of layers with different properties can achieve more precise control over the shuttling of polysulfides while providing higher ion transport rates. (3) Porous separators: Porous separators with high porosity can accom-

moderate more electrolytes, contributing to improved electrical conductivity and polysulfide adsorption capability in lithium–sulfur batteries. Researchers are exploring various pore sizes and pore structures to optimize battery performance. (4) Metal–organic framework (MOF) materials: MOFs, known for their large surface areas and porous structures, have found applications in lithium–sulfur battery separators due to their exceptional ability to adsorb polysulfides. (5) Biobased materials: Biodegradable materials, with their natural resources, renewability, and environmental friendliness, hold potential for use in eco-friendly batteries. (6) Two-dimensional materials: Two-dimensional materials such as graphene have been investigated for use in battery separators due to their excellent conductivity and mechanical strength, which could enhance battery performance. These innovative structural designs and material selections are expected to drive the commercialization of lithium–sulfur batteries in the future, playing a crucial role in energy storage systems.

Author Contributions: Conceptualization, Z.C.; investigation, X.Y., Y.Z. (Yixuan Zhao) and X.F.; writing—original draft preparation, Y.Z. (Yingbao Zhu). and H.C.; writing—review and editing, Z.C. and D.E.A. All authors have read and agreed to the published version of the manuscript.

Funding: This work was funded by the Six Talent Peaks Fund of Jiangsu Province (No. XCL-025) and Foreign Expert Introduction Program of the Ministry of Science and Technology (No. G2023014010).

Institutional Review Board Statement: Not applicable.

Data Availability Statement: Not applicable.

Conflicts of Interest: Author Hui Chen and Xuguang Fu were employed by the company of Jiangsu Zhongneng Polysilicon Technology Development Co., Ltd. The remaining authors declare that the research was conducted in the absence of any commercial or financial relationships that could be construed as a potential conflict of interest.

References

1. Kang, N.; Lin, Y.X.; Yang, L.; Lu, D.P.; Xiao, J.; Qi, Y.; Cai, M. Cathode porosity is a missing key parameter to optimize lithium-sulfur battery energy density. *Nat. Commun.* **2019**, *10*, 4597. [[CrossRef](#)]
2. Liu, M.; Deng, N.P.; Ju, J.G.; Fan, L.L.; Wang, L.Y.; Li, Z.J.; Zhao, H.J.; Yang, G.; Kang, W.M.; Yan, J.; et al. A Review: Electrospun Nanofiber Materials for Lithium-Sulfur Batteries. *Adv. Funct. Mater.* **2019**, *29*, 1905467. [[CrossRef](#)]
3. Din, M.M.U.; Murugan, R. Metal Coated Polypropylene Separator with Enhanced Surface Wettability for High Capacity Lithium Metal Batteries. *Sci. Rep.* **2019**, *9*, 16795. [[CrossRef](#)] [[PubMed](#)]
4. Jeong, Y.C.; Kim, J.H.; Nam, S.; Park, C.R.; Yang, S.J. Rational Design of Nanostructured Functional Interlayer/Separator for Advanced Li-S Batteries. *Adv. Funct. Mater.* **2018**, *28*, 1707411. [[CrossRef](#)]
5. Cuisinier, M.; Hart, C.; Balasubramanian, M.; Garsuch, A.; Nazar, L.F. Radical or Not Radical: Revisiting Lithium-Sulfur Electrochemistry in Nonaqueous Electrolytes. *Adv. Energy Mater.* **2015**, *5*, 1401801. [[CrossRef](#)]
6. Yuan, Z.; Peng, H.J.; Hou, T.Z.; Huang, J.Q.; Chen, C.M.; Wang, D.W.; Cheng, X.B.; Wei, F.; Zhang, Q. Powering Lithium-Sulfur Battery Performance by Propelling Polysulfide Redox at Sulfiphilic Hosts. *Nano Lett.* **2016**, *16*, 519–527. [[CrossRef](#)] [[PubMed](#)]
7. Song, Y.Z.; Cai, W.L.; Kong, L.; Cai, J.S.; Zhang, Q.; Sun, J.Y. Rationalizing Electrocatalysis of Li-S Chemistry by Mediator Design: Progress and Prospects. *Adv. Energy Mater.* **2020**, *10*, 1901075. [[CrossRef](#)]
8. Ren, W.C.; Ma, W.; Zhang, S.F.; Tang, B.T. Recent advances in shuttle effect inhibition for lithium sulfur batteries. *Energy Storage Mater.* **2019**, *23*, 707–732. [[CrossRef](#)]
9. Liu, H.; Lai, W.-H.; Yang, H.-L.; Zhu, Y.-F.; Lei, Y.-J.; Zhao, L.; Peng, J.; Wang, Y.-X.; Chou, S.-L.; Liu, H.-K. Efficient separators with fast Li-ion transfer and high polysulfide entrapment for superior lithium-sulfur batteries. *Chem. Eng. J.* **2021**, *408*, 127348. [[CrossRef](#)]
10. Balach, J.; Jaumann, T.; Klose, M.; Oswald, S.; Eckert, J.; Giebeler, L. Functional Mesoporous Carbon-Coated Separator for Long-Life, High-Energy Lithium-Sulfur Batteries. *Adv. Funct. Mater.* **2015**, *25*, 5285–5291. [[CrossRef](#)]
11. Manthiram, A.; Chung, S.H.; Zu, C.X. Lithium-Sulfur Batteries: Progress and Prospects. *Adv. Mater.* **2015**, *27*, 1980–2006. [[CrossRef](#)] [[PubMed](#)]
12. Wu, F.; Lee, J.T.; Magasinski, A.; Kim, H.; Yushin, G. Solution-Based Processing of Graphene–Li₂S Composite Cathodes for Lithium-Ion and Lithium–Sulfur Batteries. *Part. Part. Syst. Charact.* **2014**, *31*, 639–644. [[CrossRef](#)]
13. Gu, S.; Huang, X.; Wang, Q.; Jin, J.; Wang, Q.; Wen, Z.; Qian, R. A hybrid electrolyte for long-life semi-solid-state lithium sulfur batteries. *J. Mater. Chem. A* **2017**, *5*, 13971–13975. [[CrossRef](#)]
14. Huang, S.; Zhang, L.; Wang, J.; Zhu, J.; Shen, P.K. In situ carbon nanotube clusters grown from three-dimensional porous graphene networks as efficient sulfur hosts for high-rate ultra-stable Li–S batteries. *Nano Res.* **2018**, *11*, 1731–1743. [[CrossRef](#)]

15. Lee, W.Y.; Jin, E.M.; Cho, J.S.; Kang, D.-W.; Jin, B.; Jeong, S.M. Freestanding flexible multilayered Sulfur–Carbon nanotubes for Lithium–Sulfur battery cathodes. *Energy* **2020**, *212*, 118779. [[CrossRef](#)]
16. Chen, R.; Zhao, T.; Wu, F. From a historic review to horizons beyond: Lithium–sulfur batteries run on the wheels. *Chem. Commun.* **2015**, *51*, 18–33. [[CrossRef](#)]
17. Phung, J.; Zhang, X.Z.; Deng, W.J.; Li, G. An overview of MOF-based separators for lithium-sulfur batteries. *Sustain. Mater. Technol.* **2022**, *31*, e00374. [[CrossRef](#)]
18. Zhang, Y.S.; Zhang, X.L.; Silva, S.R.P.; Ding, B.; Zhang, P.; Shao, G.S. Lithium-Sulfur Batteries Meet Electrospinning: Recent Advances and the Key Parameters for High Gravimetric and Volume Energy Density. *Adv. Sci.* **2022**, *9*, 2103879. [[CrossRef](#)]
19. Zhang, Y.G.; Yang, S.; Zhou, S.Y.; Zhang, L.B.; Gu, B.B.; Dong, Y.Y.; Kong, S.Z.; Cai, D.; Fang, G.Y.; Nie, H.G.; et al. Oxygen doping in antimony sulfide nanosheets to facilitate catalytic conversion of polysulfides for lithium-sulfur batteries. *Chem. Commun.* **2021**, *57*, 3255–3258. [[CrossRef](#)]
20. Manthiram, A.; Fu, Y.; Su, Y.-S. Challenges and Prospects of Lithium–Sulfur Batteries. *Acc. Chem. Res.* **2013**, *46*, 1125–1134. [[CrossRef](#)]
21. Cuisinier, M.; Cabelguen, P.E.; Evers, S.; He, G.; Kolbeck, M.; Garsuch, A.; Bolin, T.; Balasubramanian, M.; Nazar, L.F. Sulfur Speciation in Li-S Batteries Determined by Operando X-ray Absorption Spectroscopy. *J. Phys. Chem. Lett.* **2013**, *4*, 3227–3232. [[CrossRef](#)]
22. Diao, Y.; Xie, K.; Xiong, S.; Hong, X. Analysis of Polysulfide Dissolved in Electrolyte in Discharge-Charge Process of Li-S Battery. *J. Electrochem. Soc.* **2012**, *159*, A421–A425. [[CrossRef](#)]
23. Wild, M.; O'Neill, L.; Zhang, T.; Purkayastha, R.; Minton, G.; Marinescu, M.; Offer, G.J. Lithium sulfur batteries, a mechanistic review. *Energy Environ. Sci.* **2015**, *8*, 3477–3494. [[CrossRef](#)]
24. Zhao, E.Y.; Nie, K.H.; Yu, X.Q.; Hu, Y.S.; Wang, F.W.; Xiao, J.; Li, H.; Huang, X.J. Advanced Characterization Techniques in Promoting Mechanism Understanding for Lithium-Sulfur Batteries. *Adv. Funct. Mater.* **2018**, *28*, 1707543. [[CrossRef](#)]
25. Sun, J.; Sun, Y.M.; Pasta, M.; Zhou, G.M.; Li, Y.Z.; Liu, W.; Xiong, F.; Cui, Y. Entrapment of Polysulfides by a Black-Phosphorus-Modified Separator for Lithium-Sulfur Batteries. *Adv. Mater.* **2016**, *28*, 9797–9803. [[CrossRef](#)] [[PubMed](#)]
26. Yao, S.S.; Cui, J.; Huang, J.Q.; Lu, Z.H.; Deng, Y.; Chong, W.G.; Wu, J.X.; Ihsan Ul Haq, M.; Ciucci, F.; Kim, J.K. Novel 2D Sb₂S₃ Nanosheet/CNT Coupling Layer for Exceptional Polysulfide Recycling Performance. *Adv. Energy Mater.* **2018**, *8*, 1800710. [[CrossRef](#)]
27. Park, J.; Kim, E.T.; Kim, C.; Pyun, J.; Jang, H.S.; Shin, J.; Choi, J.W.; Char, K.; Sung, Y.E. The Importance of Confined Sulfur Nanodomains and Adjoining Electron Conductive Pathways in Subreaction Regimes of Li-S Batteries. *Adv. Energy Mater.* **2017**, *7*, 1700074. [[CrossRef](#)]
28. Wu, J.Y.; Zeng, H.X.; Li, X.W.; Pei, H.J.; Xue, Z.G.; Ye, Y.S.; Xie, X.L. Dual-Functional Interlayer Based on Radially Oriented Ultrathin MoS₂ Nanosheets for High-Performance Lithium Sulfur-Batteries. *Acs Appl. Energy Mater.* **2019**, *2*, 1702–1711. [[CrossRef](#)]
29. Zhao, M.; Li, B.-Q.; Chen, X.; Xie, J.; Yuan, H.; Huang, J.-Q. Redox Comediation with Organopolysulfides in Working Lithium-Sulfur Batteries. *Chem* **2020**, *6*, 3297–3311. [[CrossRef](#)]
30. Zhao, M.; Peng, Y.-Q.; Li, B.-Q.; Zhang, X.-Q.; Huang, J.-Q. Regulation of carbon distribution to construct high-sulfur-content cathode in lithium–sulfur batteries. *J. Energy Chem.* **2021**, *56*, 203–208. [[CrossRef](#)]
31. Sadd, M.; De Angelis, S.; Colding-Jorgensen, S.; Blanchard, D.; Johnsen, R.E.; Sanna, S.; Borisova, E.; Matic, A.; Bowen, J.R. Visualization of Dissolution-Precipitation Processes in Lithium-Sulfur Batteries. *Adv. Energy Mater.* **2022**, *12*, 2103126. [[CrossRef](#)]
32. Ren, Y.X.; Zhao, T.S.; Liu, M.; Tan, P.; Zeng, Y.K. Modeling of lithium-sulfur batteries incorporating the effect of Li₂S precipitation. *J. Power Sources* **2016**, *336*, 115–125. [[CrossRef](#)]
33. Jayaprakash, N.; Shen, J.; Moganty, S.S.; Corona, A.; Archer, L.A. Porous Hollow Carbon@Sulfur Composites for High-Power Lithium-Sulfur Batteries. *Angew. Chem. Int. Ed.* **2011**, *50*, 5904–5908. [[CrossRef](#)] [[PubMed](#)]
34. Guo, J.; Yang, Z.; Yu, Y.; Abruna, H.D.; Archer, L.A. Lithium-sulfur battery cathode enabled by lithium-nitrile interaction. *J. Am. Chem. Soc.* **2013**, *135*, 763–767. [[CrossRef](#)] [[PubMed](#)]
35. Wang, H.; Yang, Y.; Liang, Y.; Robinson, J.T.; Li, Y.; Jackson, A.; Cui, Y.; Dai, H. Graphene-wrapped sulfur particles as a rechargeable lithium-sulfur battery cathode material with high capacity and cycling stability. *Nano Lett.* **2011**, *11*, 2644–2647. [[CrossRef](#)] [[PubMed](#)]
36. Barai, P.; Mistry, A.; Mukherjee, P.P. Poromechanical effect in the lithium–sulfur battery cathode. *Extrem. Mech. Lett.* **2016**, *9*, 359–370. [[CrossRef](#)]
37. Yan, J.H.; Liu, X.B.; Li, B.Y. Capacity Fade Analysis of Sulfur Cathodes in Lithium-Sulfur Batteries. *Adv. Sci.* **2016**, *3*, 1600101. [[CrossRef](#)]
38. He, Y.B.; Qiao, Y.; Chang, Z.; Cao, X.; Jia, M.; He, P.; Zhou, H.S. Developing A “Polysulfide-Phobic” Strategy to Restrain Shuttle Effect in Lithium-Sulfur Batteries. *Angew. Chem. Int. Ed.* **2019**, *58*, 11774–11778. [[CrossRef](#)]
39. Liu, D.H.; Zhang, C.; Zhou, G.M.; Lv, W.; Ling, G.W.; Zhi, L.J.; Yang, Q.H. Catalytic Effects in Lithium-Sulfur Batteries: Promoted Sulfur Transformation and Reduced Shuttle Effect. *Adv. Sci.* **2018**, *5*, 1700270. [[CrossRef](#)] [[PubMed](#)]
40. Wang, J.; Yi, S.; Liu, J.; Sun, S.; Liu, Y.; Yang, D.; Xi, K.; Gao, G.; Abdelkader, A.; Yan, W.; et al. Suppressing the Shuttle Effect and Dendrite Growth in Lithium-Sulfur Batteries. *ACS Nano* **2020**, *14*, 9819–9831. [[CrossRef](#)]
41. Ghazi, Z.A.; He, X.; Khattak, A.M.; Khan, N.A.; Liang, B.; Iqbal, A.; Wang, J.X.; Sin, H.S.; Li, L.S.; Tang, Z.Y. MoS₂/Celgard Separator as Efficient Polysulfide Barrier for Long-Life Lithium-Sulfur Batteries. *Adv. Mater.* **2017**, *29*, 1606817. [[CrossRef](#)]

42. Zhai, P.; Liu, K.; Wang, Z.; Shi, L.; Yuan, S. Multifunctional separators for high-performance lithium-ion batteries. *J. Power Sources* **2021**, *499*, 229973. [[CrossRef](#)]
43. Lei, T.; Chen, W.; Lv, W.; Huang, J.; Zhu, J.; Chu, J.; Yan, C.; Wu, C.; Yan, Y.; He, W.; et al. Inhibiting Polysulfide Shuttling with a Graphene Composite Separator for Highly Robust Lithium-Sulfur Batteries. *Joule* **2018**, *2*, 2091–2104. [[CrossRef](#)]
44. Gao, Z.; Xue, Z.; Miao, Y.; Chen, B.; Xu, J.; Shi, H.; Tang, T.; Zhao, X. TiO₂@Porous carbon nanotubes modified separator as polysulfide barrier for lithium-sulfur batteries. *J. Alloys Compd.* **2022**, *906*, 164249. [[CrossRef](#)]
45. Cao, R.; Xu, W.; Lv, D.; Xiao, J.; Zhang, J.-G. Anodes for Rechargeable Lithium-Sulfur Batteries. *Adv. Energy Mater.* **2015**, *5*, 1402273. [[CrossRef](#)]
46. Cheng, X.B.; Huang, J.Q.; Zhang, Q. Review-Li Metal Anode in Working Lithium-Sulfur Batteries. *J. Electrochem. Soc.* **2018**, *165*, A6058–A6072. [[CrossRef](#)]
47. Xiong, S.; Xie, K.; Diao, Y.; Hong, X. Characterization of the solid electrolyte interphase on lithium anode for preventing the shuttle mechanism in lithium-sulfur batteries. *J. Power Sources* **2014**, *246*, 840–845. [[CrossRef](#)]
48. Rong, G.L.; Zhang, X.Y.; Zhao, W.; Qiu, Y.C.; Liu, M.N.; Ye, F.M.; Xu, Y.; Chen, J.F.; Hou, Y.; Li, W.F.; et al. Liquid-Phase Electrochemical Scanning Electron Microscopy for In Situ Investigation of Lithium Dendrite Growth and Dissolution. *Adv. Mater.* **2017**, *29*, 1606187. [[CrossRef](#)]
49. Rosso, M.; Brissot, C.; Teyssot, A.; Dolle, M.; Sannier, L.; Tarascon, J.M.; Bouchet, R.; Lascaud, S. Dendrite short-circuit and fuse effect on Li/polymer/Li cells. *Electrochim. Acta* **2006**, *51*, 5334–5340. [[CrossRef](#)]
50. Fan, L.; Chen, S.H.; Zhu, J.Y.; Ma, R.F.; Li, S.P.; Podila, R.; Rao, A.M.; Yang, G.Z.; Wang, C.X.; Liu, Q.; et al. Simultaneous Suppression of the Dendrite Formation and Shuttle Effect in a Lithium-Sulfur Battery by Bilateral Solid Electrolyte Interface. *Adv. Sci.* **2018**, *5*, 1700934. [[CrossRef](#)]
51. Hu, Y.; Chen, W.; Lei, T.; Jiao, Y.; Wang, H.; Wang, X.; Rao, G.; Wang, X.; Chen, B.; Xiong, J. Graphene quantum dots as the nucleation sites and interfacial regulator to suppress lithium dendrites for high-loading lithium-sulfur battery. *Nano Energy* **2020**, *68*, 104373. [[CrossRef](#)]
52. Akhtar, N.; Sun, X.; Yasir Akram, M.; Zaman, F.; Wang, W.; Wang, A.; Chen, L.; Zhang, H.; Guan, Y.; Huang, Y. A gelatin-based artificial SEI for lithium deposition regulation and polysulfide shuttle suppression in lithium-sulfur batteries. *J. Energy Chem.* **2021**, *52*, 310–317. [[CrossRef](#)]
53. Guo, J.; Zhao, S.; He, G.; Zhang, F. Novel Synergistic Strategy for Developing High-Performance Lithium Sulfur Batteries of Large Areal Sulfur Loading by SEI Modified Separator. *ACS Appl. Energy Mater.* **2018**, *1*, 932–940. [[CrossRef](#)]
54. Li, G.; Huang, Q.; He, X.; Gao, Y.; Wang, D.; Kim, S.H.; Wang, D. Self-Formed Hybrid Interphase Layer on Lithium Metal for High-Performance Lithium-Sulfur Batteries. *ACS Nano* **2018**, *12*, 1500–1507. [[CrossRef](#)] [[PubMed](#)]
55. Guo, J.; Wen, Z.; Wu, M.; Jin, J.; Liu, Y. Vinylene carbonate–LiNO₃: A hybrid additive in carbonic ester electrolytes for SEI modification on Li metal anode. *Electrochem. Commun.* **2015**, *51*, 59–63. [[CrossRef](#)]
56. Li, N.W.; Yin, Y.X.; Yang, C.P.; Guo, Y.G. An Artificial Solid Electrolyte Interphase Layer for Stable Lithium Metal Anodes. *Adv. Mater.* **2016**, *28*, 1853–1858. [[CrossRef](#)]
57. Bruckner, J.; Thieme, S.; Bottger-Hiller, F.; Bauer, I.; Grossmann, H.T.; Strubel, P.; Althues, H.; Spange, S.; Kaskel, S. Carbon-Based Anodes for Lithium Sulfur Full Cells with High Cycle Stability. *Adv. Funct. Mater.* **2014**, *24*, 1284–1289. [[CrossRef](#)]
58. Wang, L.; Liu, J.; Yuan, S.; Wang, Y.; Xia, Y. To mitigate self-discharge of lithium-sulfur batteries by optimizing ionic liquid electrolytes. *Energy Environ. Sci.* **2016**, *9*, 224–231. [[CrossRef](#)]
59. Jin, B.; Li, Y.; Qian, J.; Zhan, X.; Zhang, Q. Environmentally Friendly Binders for Lithium-Sulfur Batteries. *ChemElectroChem* **2020**, *7*, 4158–4176. [[CrossRef](#)]
60. Zhang, S.S. Liquid electrolyte lithium/sulfur battery: Fundamental chemistry, problems, and solutions. *J. Power Sources* **2013**, *231*, 153–162. [[CrossRef](#)]
61. Li, Y.; Wang, X.; Liang, J.; Wu, K.; Xu, L.; Wang, J. Design of a high performance zeolite/polyimide composite separator for lithium-ion batteries. *Polymers* **2020**, *12*, 764. [[CrossRef](#)]
62. Li, Y.; Li, Q.; Tan, Z. A review of electrospun nanofiber-based separators for rechargeable lithium-ion batteries. *J. Power Sources* **2019**, *443*, 227262. [[CrossRef](#)]
63. Zhao, M.; Wang, J.; Chong, C.B.; Yu, X.W.; Wanga, L.L.; Shi, Z.Q. An electrospun lignin/polyacrylonitrile nonwoven composite separator with high porosity and thermal stability for lithium-ion batteries. *RSC Adv.* **2015**, *5*, 101115–101120. [[CrossRef](#)]
64. Rutledge, G.C.; Fridrikh, S.V. Formation of fibers by electrospinning. *Adv. Drug Deliv. Rev.* **2007**, *59*, 1384–1391. [[CrossRef](#)] [[PubMed](#)]
65. Gao, W.L.; Kono, J. Science and applications of wafer-scale crystalline carbon nanotube films prepared through controlled vacuum filtration. *R. Soc. Open Sci.* **2019**, *6*, 181605. [[CrossRef](#)] [[PubMed](#)]
66. Kritzer, P. Nonwoven support material for improved separators in Li-polymer batteries. *J. Power Sources* **2006**, *161*, 1335–1340. [[CrossRef](#)]
67. Zhu, J.; Ge, Y.; Kim, D.; Lu, Y.; Chen, C.; Jiang, M.; Zhang, X. A novel separator coated by carbon for achieving exceptional high performance lithium-sulfur batteries. *Nano Energy* **2016**, *20*, 176–184. [[CrossRef](#)]
68. Shao, H.; Wang, W.; Zhang, H.; Wang, A.; Chen, X.; Huang, Y. Nano-TiO₂ decorated carbon coating on the separator to physically and chemically suppress the shuttle effect for lithium-sulfur battery. *J. Power Sources* **2018**, *378*, 537–545. [[CrossRef](#)]

69. Yang, L.W.; Wang, Y.; Li, Q.; Li, Y.; Chen, Y.X.; Liu, Y.X.; Wu, Z.G.; Wang, G.K.; Zhong, B.H.; Song, Y.; et al. Inhibition of the shuttle effect of lithium-sulfur batteries via a tannic acid-metal one-step in situ chemical film-forming modified separator. *Nanoscale* **2021**, *13*, 5058–5068. [CrossRef]
70. Lin, Q.Y.; Ding, B.; Chen, S.; Li, P.; Li, Z.W.; Shi, Y.Y.; Dou, H.; Zhang, X.G. Atomic Layer Deposition of Single Atomic Cobalt as a Catalytic Interlayer for Lithium-Sulfur Batteries. *ACS Appl. Energy Mater.* **2020**, *3*, 11206–11212. [CrossRef]
71. Bhardwaj, N.; Kundu, S.C. Electrospinning: A fascinating fiber fabrication technique. *Biotechnol. Adv.* **2010**, *28*, 325–347. [CrossRef]
72. Demir, M.M.; Yilgor, I.; Yilgor, E.; Erman, B. Electrospinning of polyurethane fibers. *Polymer* **2002**, *43*, 3303–3309. [CrossRef]
73. Hao, J.; Lei, G.; Li, Z.; Wu, L.; Xiao, Q.; Wang, L. A novel polyethylene terephthalate nonwoven separator based on electrospinning technique for lithium ion battery. *J. Membr. Sci.* **2013**, *428*, 11–16. [CrossRef]
74. Zhang, L.Y.; Batchelor, W.; Varanasi, S.; Tsuzuki, T.; Wang, X.G. Effect of cellulose nanofiber dimensions on sheet forming through filtration. *Cellulose* **2012**, *19*, 561–574. [CrossRef]
75. Cho, T.-H.; Tanaka, M.; Ohnishi, H.; Kondo, Y.; Yoshikazu, M.; Nakamura, T.; Sakai, T. Composite nonwoven separator for lithium-ion battery: Development and characterization. *J. Power Sources* **2010**, *195*, 4272–4277. [CrossRef]
76. Safavi, A.; Fathi, S.; Babaei, M.R.; Mansoori, Z.; Latifi, M. Experimental and numerical analysis of fiber characteristics effects on fiber dispersion for wet-laid nonwoven. *Fibers Polym.* **2009**, *10*, 231–236. [CrossRef]
77. Wang, X.R.; Yushin, G. Chemical vapor deposition and atomic layer deposition for advanced lithium ion batteries and supercapacitors. *Energy Environ. Sci.* **2015**, *8*, 1889–1904. [CrossRef]
78. Yan, B.; Li, X.; Bai, Z.; Song, X.; Xiong, D.; Zhao, M.; Li, D.; Lu, S. A review of atomic layer deposition providing high performance lithium sulfur batteries. *J. Power Sources* **2017**, *338*, 34–48. [CrossRef]
79. Zhu, X.B.; Ouyang, Y.; Chen, J.W.; Zhu, X.G.; Luo, X.; Lai, F.L.; Zhang, H.; Miao, Y.E.; Liu, T.X. In situ extracted poly(acrylic acid) contributing to electrospun nanofiber separators with precisely tuned pore structures for ultra-stable lithium-sulfur batteries. *J. Mater. Chem. A* **2019**, *7*, 3253–3263. [CrossRef]
80. Guo, P.; Jiang, P.; Chen, W.; Qian, G.; He, D.; Lu, X. Bifunctional Al₂O₃/polyacrylonitrile membrane to suppress the growth of lithium dendrites and shuttling of polysulfides in lithium-sulfur batteries. *Electrochim. Acta* **2022**, *428*, 140955. [CrossRef]
81. Guo, Y.; Li, J.; Pitcheri, R.; Zhu, J.; Wen, P.; Qiu, Y. Electrospun Ti₄O₇/C conductive nanofibers as interlayer for lithium-sulfur batteries with ultra long cycle life and high-rate capability. *Chem. Eng. J.* **2019**, *355*, 390–398. [CrossRef]
82. Lin, Y.; Pitcheri, R.; Zhu, J.; Jiao, C.; Guo, Y.; Li, J.; Qiu, Y. Electrospun PVDF/PSSLi ionomer films as a functional separator for lithium-sulfur batteries. *J. Alloys Compd.* **2019**, *785*, 627–633. [CrossRef]
83. Feng, Y.; Wang, G.; Kang, W.; Deng, N.; Cheng, B. Taming polysulfides and facilitating lithium-ion migration: Novel electrospinning MOFs@PVDF-based composite separator with spiderweb-like structure for Li-S batteries. *Electrochim. Acta* **2021**, *365*, 137344. [CrossRef]
84. Li, Y.; Zhang, J.; Zhou, C.; Ling, M.; Lu, J.; Hou, Y.; Zhang, Q.; He, Q.; Zhan, X.; Chen, F. Flame-retardant and thermal-stable separator trapping polysulfides for lithium-sulfur battery. *J. Alloys Compd.* **2020**, *826*, 154197. [CrossRef]
85. Deng, N.; Wang, Y.; Yan, J.; Ju, J.; Li, Z.; Fan, L.; Zhao, H.; Kang, W.; Cheng, B. A F-doped tree-like nanofiber structural poly-m-phenyleneisophthalamide separator for high-performance lithium-sulfur batteries. *J. Power Sources* **2017**, *362*, 243–249. [CrossRef]
86. Zhu, Y.; Wu, X.; Li, M.; Ji, Y.; Li, Q.; He, X.; Lei, Z.; Liu, Z.; Jiang, R.; Sun, J. Synthesis of Titanium Molybdenum Nitride-Decorated Electrospun Carbon Nanofiber Membranes as Interlayers to Suppress Polysulfide Shuttling in Lithium-Sulfur Batteries. *ACS Sustain. Chem. Eng.* **2022**, *10*, 776–788. [CrossRef]
87. Du, X.; Ma, D.; Zhang, Y.; Ma, J.; Wang, J.; Xiao, Q.; Wang, B.; Tian, L.; Zhuang, J. Electrospun TiO₂ Nanofibers Featuring Surface Oxygen Vacancies as a Multifunctional Interlayer for High-Performance Lithium-Sulfur Batteries in a Wide Temperature Range. *Inorg. Chem.* **2023**, *62*, 5134–5144. [CrossRef] [PubMed]
88. Jiang, X.; Zhang, S.; Zou, B.; Li, G.; Yang, S.; Zhao, Y.; Lian, J.; Li, H.; Ji, H. Electrospun CoSe@NC nanofiber membrane as an effective polysulfides adsorption-catalysis interlayer for Li-S batteries. *Chem. Eng. J.* **2022**, *430*, 131911. [CrossRef]
89. Huangfu, Y.; Zheng, T.; Zhang, K.; She, X.; Xu, H.; Fang, Z.; Xie, K. Facile fabrication of permselective g-C₃N₄ separator for improved lithium-sulfur batteries. *Electrochim. Acta* **2018**, *272*, 60–67. [CrossRef]
90. Feng, P.; Hou, W.; Bai, Z.; Bai, Y.; Sun, K.; Wang, Z. Ultrathin two-dimensional bimetal NiCo-based MOF nanosheets as ultralight interlayer in lithium-sulfur batteries. *Chin. Chem. Lett.* **2023**, *34*, 107427. [CrossRef]
91. Li, W.; Wang, S.; Fan, Z.; Li, S.; Bernussi, A.; Newman, N. Functionalized bacterial cellulose as a separator to address polysulfides shuttling in lithium-sulfur batteries. *Mater. Today Energy* **2021**, *21*, 100813. [CrossRef]
92. Zhang, Z.; Wang, G.; Lai, Y.; Li, J. A freestanding hollow carbon nanofiber/reduced graphene oxide interlayer for high-performance lithium-sulfur batteries. *J. Alloys Compd.* **2016**, *663*, 501–506. [CrossRef]
93. Zheng, B.; Yu, L.; Zhao, Y.; Xi, J. Ultralight carbon flakes modified separator as an effective polysulfide barrier for lithium-sulfur batteries. *Electrochim. Acta* **2019**, *295*, 910–917. [CrossRef]
94. Liu, Q.; Han, X.T.; Dou, Q.Y.; Xiong, P.X.; Kang, Y.B.; Kang, S.W.; Kim, B.K.; Park, H.S. Multiphase and Multicomponent Nickel-Iron Oxide Heterostructure as an Efficient Separator Modification Layer for Advanced Lithium Sulfur Batteries. *Batter. Supercaps* **2021**, *4*, 1843–1849. [CrossRef]
95. Tian, M.; Pei, F.; Yao, M.; Fu, Z.; Lin, L.; Wu, G.; Xu, G.; Kitagawa, H.; Fang, X. Ultrathin MOF nanosheet assembled highly oriented microporous membrane as an interlayer for lithium-sulfur batteries. *Energy Storage Mater.* **2019**, *21*, 14–21. [CrossRef]

96. Sung, S.; Kim, B.H.; Lee, S.; Choi, S.; Yoon, W.Y. Increasing sulfur utilization in lithium-sulfur batteries by a Co-MOF-74@MWCNT interlayer. *J. Energy Chem.* **2021**, *60*, 186–193. [[CrossRef](#)]
97. Meng, L.; Li, Y.; Lin, Q.X.; Long, J.; Wang, Y.; Hu, J. Nitrogen and Oxygen Dual Self-Doped Flexible PPTA Nanofiber Carbon Paper as an Effective Interlayer for Lithium-Sulfur Batteries. *ACS Appl. Energy Mater.* **2021**, *4*, 8592–8603. [[CrossRef](#)]
98. Li, Y.; Meng, L.; Jin, L.; Yun, L.; Jian, H. A wet-laid carbon paper with 3D conductive structure as an interlayer for lithium-sulfur batteries. *Mater. Res. Express* **2019**, *6*, 125547. [[CrossRef](#)]
99. Chong, W.G.; Xiao, F.; Yao, S.S.; Cui, J.; Sadighi, Z.; Wu, J.X.; Ihsan-Ul-Haq, M.; Shao, M.H.; Kim, J.K. Nitrogen-doped graphene fiber webs for multi-battery energy storage. *Nanoscale* **2019**, *11*, 6334–6342. [[CrossRef](#)]
100. Suriyakumar, S.; Stephan, A.M. Mitigation of Polysulfide Shuttling by Interlayer/Permselective Separators in Lithium-Sulfur Batteries. *ACS Appl. Energy Mater.* **2020**, *3*, 8095–8129. [[CrossRef](#)]
101. Chong, W.G.; Huang, J.Q.; Xu, Z.L.; Qin, X.Y.; Wang, X.Y.; Kim, J.K. Lithium-Sulfur Battery Cable Made from Ultralight, Flexible Graphene/Carbon Nanotube/Sulfur Composite Fibers. *Adv. Funct. Mater.* **2017**, *27*, 1604815. [[CrossRef](#)]
102. Chong, W.G.; Xiao, Y.; Huang, J.-Q.; Yao, S.; Cui, J.; Qin, L.; Gao, C.; Kim, J.-K. Highly conductive porous graphene/sulfur composite ribbon electrodes for flexible lithium-sulfur batteries. *Nanoscale* **2018**, *10*, 21132–21141. [[CrossRef](#)]
103. Zhang, S.M.; Shi, H.D.; Tang, J.W.; Shi, W.X.; Wu, Z.S.; Wang, X. Super-aligned films of sub-1 nm Bi₂O₃-polyoxometalate nanowires as interlayers in lithium-sulfur batteries. *Sci. China-Mater.* **2021**, *64*, 2949–2957. [[CrossRef](#)]
104. Wang, J.; Wu, T.; Zhang, S.; Gu, S.; Jin, J.; Wen, Z. Metal-organic-framework-derived N-C-Co film as a shuttle-suppressing interlayer for lithium-sulfur battery. *Chem. Eng. J.* **2018**, *334*, 2356–2362. [[CrossRef](#)]
105. Zhang, Z.; Lai, Y.; Zhang, Z.; Zhang, K.; Li, J. Al₂O₃-coated porous separator for enhanced electrochemical performance of lithium sulfur batteries. *Electrochim. Acta* **2014**, *129*, 55–61. [[CrossRef](#)]
106. Hu, X.; Huang, T.; Wang, S.; Lin, S.; Feng, Z.; Chung, L.-H.; He, J. Separator modified by Co-porphyrin based Zr-MOF@CNT composite enabling efficient polysulfides catalytic conversion for advanced lithium-sulfur batteries. *Electrochim. Acta* **2021**, *398*, 139317. [[CrossRef](#)]
107. Ma, B.; Gao, Y.; Niu, M.; Luo, M.; Li, H.; Bai, Y.; Sun, K. ZIF-67/Super P modified separator as an efficient polysulfide barrier for high-performance lithium-sulfur batteries. *Solid State Ion.* **2021**, *371*, 115750. [[CrossRef](#)]
108. Wang, Z.; Feng, M.; Sun, H.; Li, G.; Fu, Q.; Li, H.; Liu, J.; Sun, L.; Mauger, A.; Julien, C.M.; et al. Constructing metal-free and cost-effective multifunctional separator for high-performance lithium-sulfur batteries. *Nano Energy* **2019**, *59*, 390–398. [[CrossRef](#)]
109. Zhao, Q.; Zhu, Q.; An, Y.; Chen, R.; Sun, N.; Wu, F.; Xu, B. A 3D conductive carbon interlayer with ultrahigh adsorption capability for lithium-sulfur batteries. *Appl. Surf. Sci.* **2018**, *440*, 770–777. [[CrossRef](#)]
110. Li, W.; Ye, Y.; Qian, J.; Xing, Y.; Qu, W.; Zhang, N.; Li, L.; Wu, F.; Chen, R. Oxygenated Nitrogen-Doped Microporous Nanocarbon as a Permselective Interlayer for Ultrastable Lithium-Sulfur Batteries. *ChemElectroChem* **2019**, *6*, 1094–1100. [[CrossRef](#)]
111. Lu, X.; Wang, H.; Liu, X.; Song, Z.; Jiang, N.; Xie, F.; Zheng, Q.; Lin, D. Functional separators prepared via in-situ growth of hollow CoSO₄ hydrate arrays on pristine polypropylene membrane for high performance lithium-Sulfur batteries. *J. Alloys Compd.* **2020**, *838*, 155618. [[CrossRef](#)]
112. Li, J.; Jiao, C.; Zhu, J.; Zhong, L.; Kang, T.; Aslam, S.; Wang, J.; Zhao, S.; Qiu, Y. Hybrid co-based MOF nanoboxes/CNFs interlayer as microreactors for polysulfides-trapping in lithium-sulfur batteries. *J. Energy Chem.* **2021**, *57*, 469–476. [[CrossRef](#)]
113. Liu, J.W.; Wang, J.A.; Zhu, L.; Chen, X.; Yi, G.; Ma, Q.Y.; Sun, S.Y.; Wang, N.; Cui, X.M.; Chai, Q.Q.; et al. In situ grown MOFs and PVDF-HFP co-modified aramid gel nanofiber separator for high-safety lithium-sulfur batteries. *J. Mater. Chem. A* **2022**, *10*, 14098–14110. [[CrossRef](#)]
114. Zhang, F.; Gao, Y.; Wu, F.; Li, L.; Li, J.; Wang, G. Constructing MIL-101(Cr) membranes on carbon nanotube films as ion-selective interlayers for lithium-sulfur batteries. *Nanotechnology* **2022**, *33*, 215401. [[CrossRef](#)]
115. Wang, X.; Wang, Y.; Wu, F.; Jin, G.; Li, J.; Zhang, Z. Continuous zirconium-based MOF-808 membranes for polysulfide shuttle suppression in lithium-sulfur batteries. *Appl. Surf. Sci.* **2022**, *596*, 153628. [[CrossRef](#)]
116. Yi, R.; Liu, C.; Zhao, Y.; Hardwick, L.J.; Li, Y.; Geng, X.; Zhang, Q.; Yang, L.; Zhao, C. A light-weight free-standing graphene foam-based interlayer towards improved Li-S cells. *Electrochim. Acta* **2019**, *299*, 479–488. [[CrossRef](#)]
117. Han, X.; Xu, Y.; Chen, X.; Chen, Y.-C.; Weadock, N.; Wan, J.; Zhu, H.; Liu, Y.; Li, H.; Rubloff, G.; et al. Reactivation of dissolved polysulfides in Li-S batteries based on atomic layer deposition of Al₂O₃ in nanoporous carbon cloth. *Nano Energy* **2013**, *2*, 1197–1206. [[CrossRef](#)]
118. Kong, W.; Wang, D.; Yan, L.; Luo, Y.; Jiang, K.; Li, Q.; Zhang, L.; Lu, S.; Fan, S.; Li, J.; et al. Ultrathin HfO₂-modified carbon nanotube films as efficient polysulfide barriers for Li-S batteries. *Carbon* **2018**, *139*, 896–905. [[CrossRef](#)]
119. Ding, H.; Zhang, Q.; Liu, Z.; Wang, J.; Ma, R.; Fan, L.; Wang, T.; Zhao, J.; Ge, J.; Lu, X.; et al. TiO₂ quantum dots decorated multi-walled carbon nanotubes as the multifunctional separator for highly stable lithium sulfur batteries. *Electrochim. Acta* **2018**, *284*, 314–320. [[CrossRef](#)]
120. Moon, S.-H.; Kim, M.-C.; Choi, J.-H.; Kim, Y.-S.; Kim, H.; Park, K.-W. 1T-MoS₂/carbon nanofiber composite as an interlayer fabricated by an in situ electrochemical fabrication method for lithium-sulfur batteries. *J. Alloys Compd.* **2021**, *857*, 158236. [[CrossRef](#)]
121. Leng, X.; Zeng, J.; Yang, M.; Li, C.; Vattikuti, S.V.P.; Chen, J.; Li, S.; Shim, J.; Guo, T.; Ko, T.J. Bimetallic Ni-Co MOF@PAN modified electrospun separator enhances high-performance lithium-sulfur batteries. *J. Energy Chem.* **2023**, *82*, 484–496. [[CrossRef](#)]

122. Kiai, M.S.; Eroglu, O.; Kizil, H. Electrospun nanofiber polyacrylonitrile coated separators to suppress the shuttle effect for long-life lithium–sulfur battery. *J. Appl. Polym. Sci.* **2020**, *137*, 48606. [[CrossRef](#)]
123. Huang, Y.; Wang, Y.; Fu, Y. A thermoregulating separator based on black phosphorus/MOFs heterostructure for thermo-stable lithium-sulfur batteries. *Chem. Eng. J.* **2023**, *454*, 140250. [[CrossRef](#)]
124. Wang, H.; Xu, C.; Du, X.; Liu, G.; Han, W.; Li, J. Ordered porous metal oxide embedded dense carbon network design as high-performance interlayer for stable lithium-sulfur batteries. *Chem. Eng. J.* **2023**, *471*, 144338. [[CrossRef](#)]
125. Wang, L.; He, Y.-B.; Shen, L.; Lei, D.; Ma, J.; Ye, H.; Shi, K.; Li, B.; Kang, F. Ultra-small self-discharge and stable lithium-sulfur batteries achieved by synergetic effects of multicomponent sandwich-type composite interlayer. *Nano Energy* **2018**, *50*, 367–375. [[CrossRef](#)]

Disclaimer/Publisher’s Note: The statements, opinions and data contained in all publications are solely those of the individual author(s) and contributor(s) and not of MDPI and/or the editor(s). MDPI and/or the editor(s) disclaim responsibility for any injury to people or property resulting from any ideas, methods, instructions or products referred to in the content.